Fisheries and Oceans Canada / Pêches et Océans Canada
Ecosystems and Oceans Science / Sciences des écosystèmes et des océans

Canadian Science Advisory Secretariat (CSAS)

Research Document 2022/040

Newfoundland and Labrador Region

Physical Oceanographic Conditions on the Newfoundland and Labrador Shelf during 2021

F. Cyr, S. Snook, C. Bishop, P.S. Galbraith, N. Chen, and G. Han

Science Branch
Fisheries and Oceans Canada
PO Box 5667
St. John's, NL A1C 5X1

June 2022

Canada

Foreword

This series documents the scientific basis for the evaluation of aquatic resources and ecosystems in Canada. As such, it addresses the issues of the day in the time frames required and the documents it contains are not intended as definitive statements on the subjects addressed but rather as progress reports on ongoing investigations.

Published by:

Fisheries and Oceans Canada
Canadian Science Advisory Secretariat
200 Kent Street
Ottawa ON K1A 0E6

http://www.dfo-mpo.gc.ca/csas-sccs/
csas-sccs@dfo-mpo.gc.ca

ISSN 1919-5044
ISBN 978-0-660-43821-4 Cat. No. Fs70-5/2022-040E-PDF

Correct citation for this publication:

Cyr, F., Snook, S., Bishop, C., Galbraith, P.S., Chen, N., and Han, G. 2022. Physical Oceanographic Conditions on the Newfoundland and Labrador Shelf during 2021. DFO Can. Sci. Advis. Sec. Res. Doc. 2022/040. iv + 48 p.

Aussi disponible en français :

Cyr, F., Snook, S., Bishop, C., Galbraith, P.S., Chen, N. et Han, G. 2022. Conditions océanographiques physiques sur le plateau continental de Terre-Neuve-et-Labrador en 2021. Secr. can. des avis sci. du MPO. Doc. de rech. 2022/040. iv + 51 p.

TABLE OF CONTENTS

ABSTRACT

An overview of physical oceanographic conditions in the Newfoundland and Labrador (NL) Region during 2021 is presented in support of the Atlantic Zone Monitoring Program (AZMP). The winter North Atlantic Oscillation (NAO) index, a key indicator of the direction and intensity of the winter wind field patterns over the Northwest (NW) Atlantic, was negative after seven consecutive years on the positive side (colder conditions), including a record high value in 2015. The large majority of the environmental parameters presented in this report were above normal (defined as the average over the 1991–2020 climatological period). The annual average air temperature at five sites around the NW Atlantic was above normal, including a record-high in Bonavista. When considering the winter period, record-highs warm temperatures were established at Iqaluit, Bonavista and St. John’s, and the second warmest winter on record was observed in Cartwright. The sea-ice season volume and area across the Newfoundland and Labrador Shelf was at its third lowest level (after 2010 and 2011) since the beginning of the time series in 1969. Only one iceberg was observed drifting south of 48°N. Ice-free seasons sea surface temperatures (SSTs) across the NW Atlantic were slightly warmer than normal. Observations from the summer AZMP oceanographic survey indicate that the cold intermediate layer (CIL) area along Seal Island, Bonavista Bay and Flemish Cap section was at its third lowest (indicating warm conditions) since 1950 (after 1965 and 1966). This contrast with 2014–17 where the volume was above normal (cold conditions). Spatially-averaged bottom temperatures in Northwest Atlantic Fisheries Organization (NAFO) divisions 3Ps (spring) and 2J3K (fall) were at their second warmest since 1980, including a record in 3Ps. The transport on the Scotian Slope in 2021 remained below normal for eight consecutive years at -1.4 standard deviation (SD). The NL climate index was at a record-high in 2021 (tied with 2010 and 1966).

INTRODUCTION

This manuscript presents an overview of the 2021 environmental and physical oceanographic conditions in the Newfoundland and Labrador (NL) Region (Figure 1), in support of the Fisheries and Oceans Canada (DFO) Atlantic Zone Monitoring Program (AZMP; Therriault et al. 1998). This report complements similar reviews of the environmental conditions in the Gulf of St. Lawrence (Galbraith et al. in prep[1]) and the Scotian Shelf and Gulf of Maine (Hebert et al. in prep[2]). Physical oceanographic conditions for the NL region in 2019 were presented in Cyr et al. (2021), while the conditions for 2020 were presented in an academic peer-review publication (Cyr and Galbraith 2021).

The information presented in this report is derived from various sources:

1. Observations made throughout the year at monitoring Station 27 near St. John's, NL;
2. Measurements made along standard AZMP cross-shelf sections (see map Figure 1);
3. Oceanographic observations made during spring and fall multi-species resource assessment surveys;
4. Sea Surface Temperatures (SSTs) from Galbraith et al. (2021). These correspond to a blend of Advanced Very High Resolution Radiometer (AVHRR) data from Pathfinder version 5.3 (1982–2014), the Maurice Lamontagne Institute (1985–2013) and the Bedford Institute of Oceanography (1997–2021).
5. Other multi-source historical data (ships of opportunity, international campaigns, surveys from other DFO regions, the Argo program, etc.);
6. Ice data from the Canadian Ice Service, while meteorological data are from Environment and Climate Change (ECCC) Canada and other sources cited in the text.

Unless otherwise specified, the data are available from DFO's Marine Environmental Data Section (MEDS) archives, and maintained in a regional data archive at the Northwest Atlantic Fisheries Centre (NAFC) in St. John's, NL.

Time series of temperature, salinity and other climate indices anomalies were constructed by subtracting the average computed over a standard climatological period from 1991 to 2020. When a variable is measured throughout the seasonal cycle (e.g. air temperature, station 27 observations), the annual anomaly is calculated as the average of monthly anomalies. Unless otherwise specified, annual or seasonal anomalies were normalized by dividing the values by the standard deviation (SD) of the data time series over the climatological period. A value of 2, for example, indicates that the index was 2 SD higher than its long-term average. As a general guide, anomalies within ±0.5 SD are considered to be normal.

The normalized values of water properties and derived climate indices are presented as "scorecards", which are color-coded gradations of 0.5 SD (Figure 2). Shades of blue represent cold environmental conditions and red represent warm conditions. In some instances, such as for the North Atlantic Oscillation (NAO), or for ice and cold intermediate layer (CIL) properties,

[1] Galbraith, P.S., Chassé, J., Dumas, J., Shaw, J.-L., Caverhill, C., Lefaivre, D. and Lafleur, C. In Prep. Physical Oceanographic Conditions in the Gulf of St. Lawrence during 2021. DFO Can. Sci. Advis. Sec. Res. Doc. 2022/034.

[2] Hebert, D., Layton, C. and Brickman, D. In Prep. Physical Oceanographic Conditions on the Scotian Shelf and in the Gulf of Maine during 2021. DFO Can. Sci. Advis. Sec. Res. Doc.

negative anomalies indicate warm conditions, and are therefore colored red. Most of the colormaps used in this report are taken from the *cmocean* colormaps package for oceanography (Thyng et al. 2016).

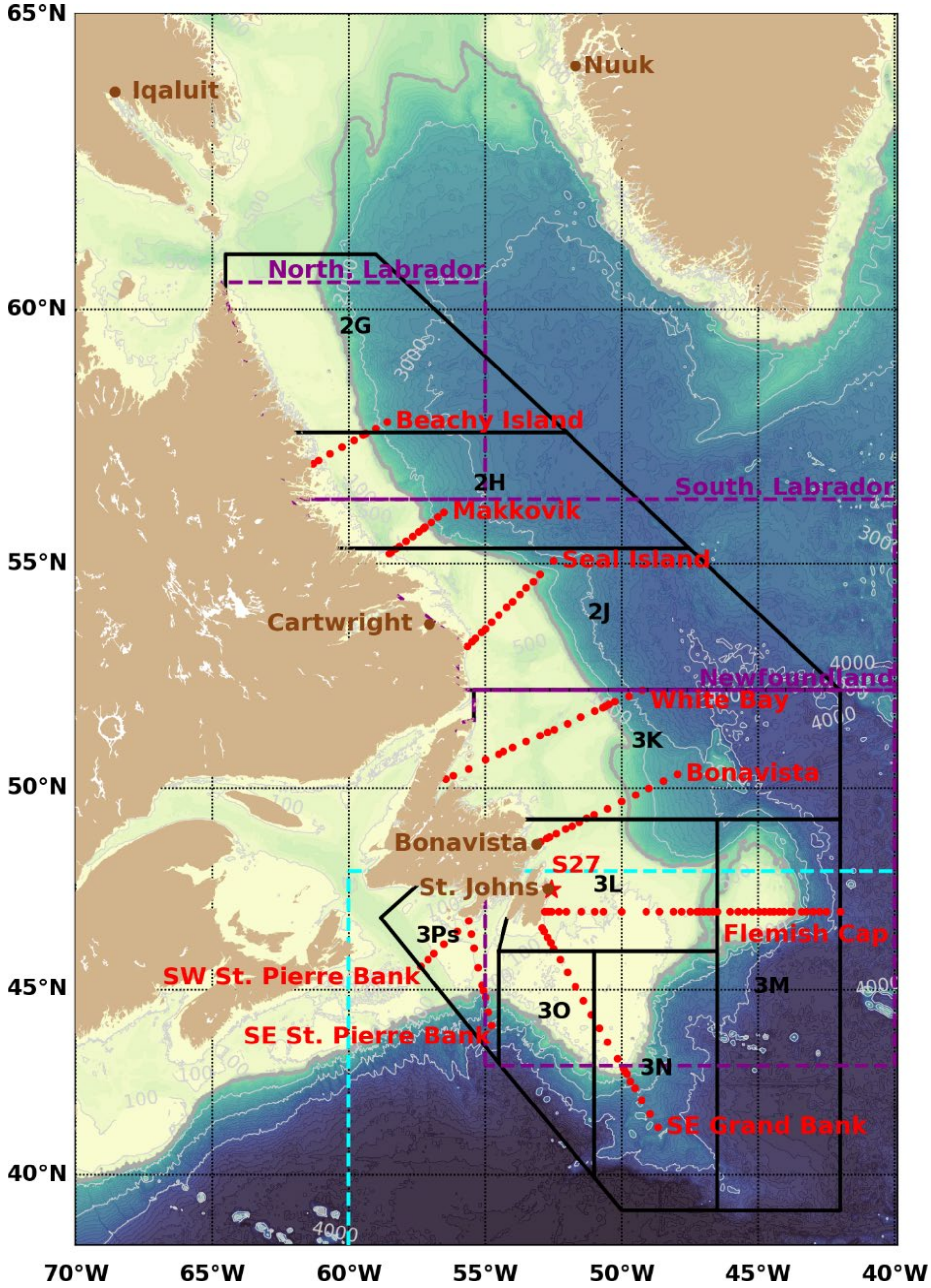

Figure 1: Map of the Northwest Atlantic ocean, including important bathymetric features (the gray isobaths are identified on the figure). NAFO Divisions (sub-areas 2 and 3) on the Newfoundland and Labrador (NL) shelf are drawn. (black boxes) The AZMP hydrographic sections are shown with red dots, and their names labeled in red text on the figure. Long-term AZMP hydrographic Station 27 is highlighted with a red star. The five stations used for the air temperature time series are shown in brown. The three regions used for sea ice calculations (Northern Labrador shelf, Southern Labrador shelf and Newfoundland shelf) are drawn with dashed magenta lines. The region used by the International Ice Patrol for iceberg sightings south of 48°N is drawn in dashed cyan. The shelf break is delimited by a thicker and darker gray contour corresponding to the isobath 1,000 m (used to clip the SST and bottom temperature).

< -3.0	-2.9 to -2.5	-2.4 to -2.0	-1.9 to -1.5	-1.4 to -1.0	-0.9 to -0.5	-0.4 to 0.0	0.0 to 0.4	0.5 to 0.9	1.0 to 1.4	1.5 to 1.9	2.0 to 2.4	2.5 to 2.9	> 3.0

Figure 2: Color scale used for the presentation of normalized anomalies. Color levels are incremented by 0.5 standard deviations (SD), where blue is below normal and red above normal. Values between 0 and ±0.5 SD remain white indicating normal conditions. Anomalies are rounded to the nearest tenth.

METEOROLOGICAL CONDITIONS

The North Atlantic Oscillation (NAO; see Figure 3 for time series since 1951 and Figure 4 for tabulated values since 1980) refers to the anomaly in the sea-level pressure (SLP) difference between the sub-tropical high (average location near the Azores) and the subpolar low (average location near Iceland). Several definitions of the NAO exist, though the one used here is from the National Center for Environmental Information of the National Oceanic and Atmospheric Administration (NOAA) available online. The winter NAO (defined here as the average of monthly values from December to March) is considered a measure of the strength of the winter westerly and northwesterly winds over the Northwest Atlantic. A high NAO index (positive phase) occurs during an intensification of the Icelandic Low and Azores High. Except for some years for which the SLP patterns are spatially shifted (e.g., 1999, 2000, and 2018), positive winter NAO years favor strong northwesterly winds, cold air and sea surface temperatures (SSTs), and heavy ice conditions on the NL shelves (Colbourne et al. 1994; Drinkwater 1996; Petrie et al. 2007). In 2021, the winter NAO was negative for the first time in seven years (although only very slightly at -0.1; first row in Figure 4). While the lowest winter NAO index value was reached in 2010, all years between 2012 and 2020 (except 2013) were positive, including the record high of +1.6 in 2015. As we will see during this report, the return to a negative winter NAO index in 2021 was accompanied by a warmer than usual winter, which had important consequences for the region as a large number of variables analyzed here were warmer than normal.

The Arctic Oscillation (AO) is a larger scale index intimately linked with the NAO. During a positive phase, the Arctic air outflow to the Northwest Atlantic increases, resulting in colder winter air temperatures over much of NL and adjacent shelf regions. Similar to the NAO, the AO was slightly negative in 2021 at -0.1 (Figure 4), indicative of warmer than usual air temperatures above the region. In 2015, the AO was at its highest value since 1990 at +1.6. A record low was reached in 2010 when it was below normal at -1.5 (warm air temperatures).

The Atlantic Multidecadal Oscillation (AMO) is also provided in Figure 4. This index, based on the Sea Surface Temperature of the Atlantic Ocean, evolves as part of a 65–80 year cycle that influences the regional climate and has consequences on the ocean circulation in the North Atlantic (e.g., Kerr 2000). The AMO has been in a positive phase since the late 1990s.

Air temperature anomalies (winter and annual values) from five coastal communities around the Northwest Atlantic (Nuuk, Greenland; Iqaluit on Baffin Island, Nunavut; Cartwright, Labrador; Bonavista and St. John's in Newfoundland; see Figure 1) are shown in Figure 4 as normalized anomalies between 1980 and 2021, and in Figure 5 and Figure 6 as annual and monthly (cumulative for all stations) anomalies, respectively. Except for Nuuk for which data are obtained from the Danish Meteorological Institute, the air temperature data from Canadian sites are from the second generation of Adjusted and Homogenized Canadian Climate Data (AHCCD), which accounts for shifts in station location and changes in observation methods (Vincent et al. 2012). Because the AHCCD product was not ready for the year 2021, historical data from the Government of Canada Monthly Climate Summaries have been used for that year.

Overall, the air temperature was above normal for all sites in 2021 (Figure 4). Temperatures were especially warm during the winter at the northern Canadian sites, being, for example, 7.8°C and 7.2°C above normal in Iqaluit, respectively for January and February, and 6.4°C and 5.0°C above normal for the same months in Cartwright (Figure 6). Over the winter season, Nuuk temperature was 0.9 SD above normal and the four Canadian sites were 2.0 to 2.4 SD above normal (Figure 4). Note that this set new records for Iqaluit, Bonavista and St. John's (tied with 2011). For Cartwright, 2021 was the second warmest winter after 2010. For the rest of the year, temperatures were still mostly on the warm side, but closer to the normal, except for July in St. John's that was cold at -1.0 SD (Figure 6). Averaged over the year the air temperatures were above normal at all sites (Figure 4, bottom row), making 2021 the second warmest year since 1950 at +1.3 SD (Figure 6). 2010 was the warmest year at +2.1 SD.

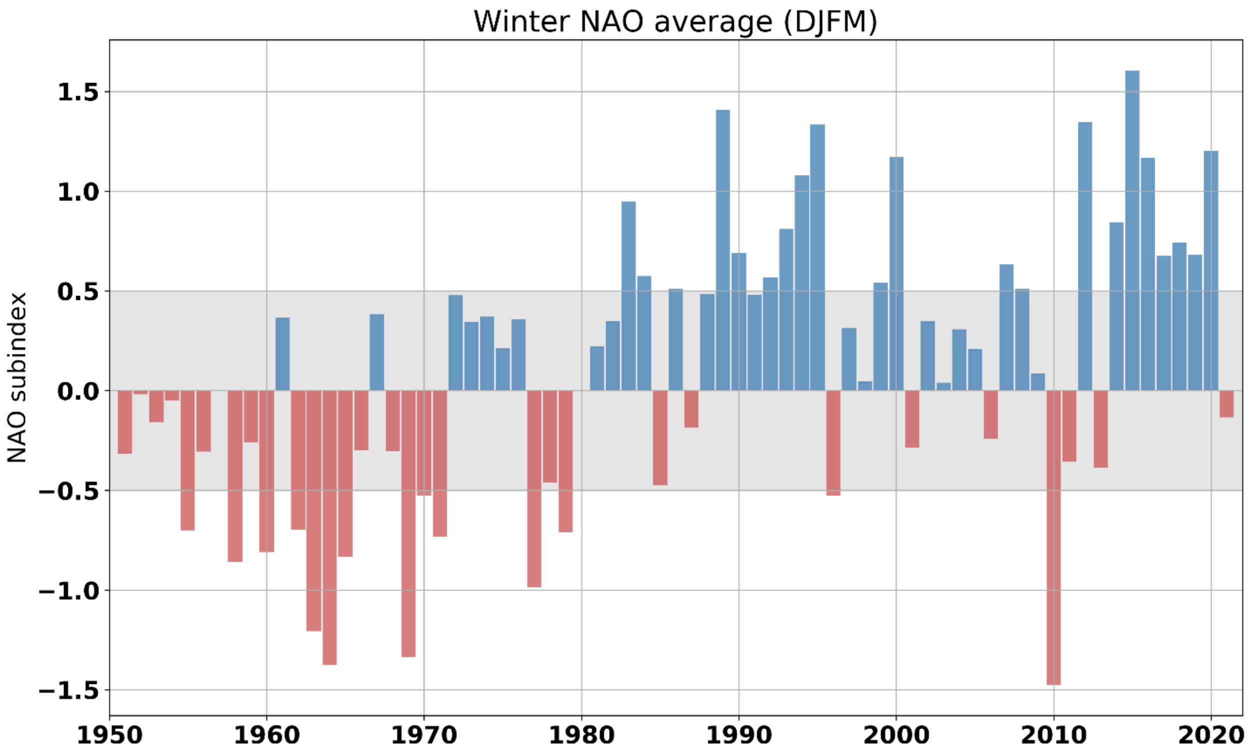

Figure 3: Winter North Atlantic Oscillation (NAO) Index calculated by averaging the December to March values since 1951 (which correspond to the average of December 1950 and January-March 1951). The NAO Index used here is from the National Center for Environmental Information of the NOAA. This index is used as part of the NL climate index mentioned in the summary (Figure 40).

	80	81	82	83	84	85	86	87	88	89	90	91	92	93	94	95	96	97	98	99
-- Climate indices --																				
NAO_{winter}	0.0	0.2	0.3	0.9	0.6	-0.5	0.5	-0.2	0.5	1.4	0.7	0.5	0.6	0.8	1.1	1.3	-0.5	0.3	0.0	0.5
AO	-0.6	-0.4	0.3	0.0	-0.2	-0.5	0.1	-0.5	0.0	1.0	1.0	0.2	0.4	0.1	0.5	-0.3	-0.5	0.0	-0.3	0.1
AMO	0.0	-0.1	-0.2	-0.1	-0.2	-0.3	-0.3	0.0	0.0	-0.1	-0.1	-0.2	-0.2	-0.2	-0.2	0.1	-0.1	0.0	0.3	0.1
-- Winter Air Temperature --																				
Nuuk	0.8	0.2	0.0	-3.0	-3.6	0.4	2.2	-0.4	0.4	-1.4	-0.6	-1.1	-1.4	-2.5	-0.7	-1.3	0.4	0.1	-0.1	-0.3
Iqaluit	0.4	0.8	0.9	-2.3	-2.0	0.6	1.7	-1.3	-0.4	-1.7	-1.1	-1.7	-0.9	-2.1	-0.8	-0.2	0.2	0.1	-1.9	-0.3
Cartwright	0.4	0.8	0.1	-1.3	-1.0	-0.2	0.0	-0.2	-0.1	-1.3	-1.3	-1.4	-1.6	-1.5	-1.1	-0.8	0.4	0.1	0.7	0.3
Bonavista	-0.3	0.6	-0.2	-0.3	-0.4	-1.0	-0.5	-0.9	-0.2	-1.5	-2.4	-1.5	-1.8	-2.1	-1.7	-1.0	0.4	-0.2	0.1	0.8
StJohns	-0.6	0.6	-0.4	0.6	0.4	-0.8	-0.3	-1.3	-0.4	-1.7	-2.4	-1.3	-1.9	-1.9	-1.5	-1.0	0.1	-0.1	-0.1	1.1
-- Annual Air Temperature --																				
Nuuk	0.4	-0.2	-1.6	-2.4	-2.7	1.0	-0.2	-0.4	0.0	-1.7	-1.2	-0.7	-2.0	-2.2	-1.1	-0.6	0.1	-0.2	0.0	-0.3
Iqaluit	0.4	1.2	-1.3	-2.1	-1.6	0.9	-1.1	-1.2	-0.4	-1.6	-1.7	-0.9	-2.3	-2.3	-0.7	0.3	0.3	0.6	-0.2	-0.5
Cartwright	-0.2	0.9	-1.3	-0.6	-1.1	-0.7	-1.0	0.3	-0.4	-0.6	-1.2	-1.5	-1.3	-1.3	-0.6	-0.5	0.3	-0.4	0.5	0.8
Bonavista	-1.1	0.6	-1.0	0.1	-0.4	-1.3	-0.9	-0.3	0.2	-0.2	-0.7	-1.7	-1.7	-1.6	-0.6	-0.7	0.5	-0.9	0.6	0.5
StJohns	-1.6	0.8	-1.3	0.3	0.1	-2.0	-1.3	-0.9	-0.1	-0.9	-0.8	-1.8	-2.2	-1.8	-0.7	-1.0	0.1	-1.4	0.4	1.8

	00	01	02	03	04	05	06	07	08	09	10	11	12	13	14	15	16	17	18	19	20	21	x̄	sd
-- Climate indices --																								
NAO_{winter}	1.2	-0.3	0.4	0.0	0.3	0.2	-0.2	0.6	0.5	0.1	-1.5	-0.4	1.3	-0.4	0.8	1.6	1.2	0.7	0.7	0.7	1.2	-0.1		
AO	0.0	-0.2	0.1	0.2	-0.2	-0.4	0.1	0.3	0.2	-0.3	-1.0	0.5	-0.2	0.0	-0.1	0.6	-0.1	0.3	0.2	-0.1	0.8	-0.1		
AMO	0.0	0.1	0.0	0.2	0.2	0.3	0.2	0.1	0.1	0.0	0.3	0.1	0.2	0.1	0.1	0.1	0.3	0.3	0.0	0.1	0.3	0.2		
-- Winter Air Temperature --																								
Nuuk	0.1	0.2	0.1	0.9	1.3	0.3	0.6	1.0	-1.5	0.6	2.3	1.3	-0.1	0.5	0.1	-1.0	0.1	0.1	-0.5	1.1	-0.5	0.9	-7.2	2.2
Iqaluit	0.2	0.4	-0.2	0.3	0.8	-0.6	0.4	1.1	-1.0	-0.1	2.2	2.1	0.6	0.6	0.5	-1.2	0.2	0.4	0.1	0.6	0.3	2.4	-23.9	3.0
Cartwright	0.2	-0.1	0.3	0.1	1.6	-0.1	0.6	0.8	-0.9	0.1	2.7	2.0	0.0	0.8	-0.8	-1.2	0.3	-0.2	0.2	-0.3	-0.9	2.2	-12.0	2.6
Bonavista	1.0	-0.3	0.1	-0.9	0.9	0.4	1.5	0.2	-0.5	0.4	1.0	1.9	0.8	0.6	-1.2	0.1	0.6	0.0	1.1	-0.7	0.0	2.0	-3.2	1.3
StJohns	1.2	-0.8	0.0	-1.0	0.7	0.5	1.4	-0.1	-0.4	0.9	0.9	2.0	0.7	0.4	-1.0	0.5	0.6	-0.1	1.2	-0.8	0.0	2.0	-3.0	1.2
-- Annual Air Temperature --																								
Nuuk	0.1	0.5	-0.1	1.1	0.4	1.0	0.6	0.4	-0.1	0.3	2.8	-0.6	0.9	0.5	0.1	-1.5	1.0	0.2	-0.9	1.0	-0.6	0.8	-1.0	1.3
Iqaluit	0.2	0.4	-0.5	0.6	-0.2	0.7	1.3	-0.1	-0.4	0.2	2.9	0.3	0.4	0.0	0.2	-1.7	0.1	0.5	-0.6	0.9	0.5	1.5	-8.3	1.5
Cartwright	0.4	0.5	-0.4	0.3	0.9	0.7	1.5	0.0	0.0	0.3	2.2	0.5	1.1	0.4	-0.1	-3.0	-0.4	0.1	-0.2	-1.1	0.4	1.5	0.2	1.4
Bonavista	0.9	0.5	-0.2	0.2	0.7	0.8	1.2	0.6	0.4	0.2	1.3	-1.6	1.4	0.7	-0.1	-0.7	0.3	0.9	-2.1	-0.5	0.9	1.6	5.0	1.0
StJohns	0.8	0.1	-0.7	0.1	0.3	0.5	1.4	-0.4	0.6	0.7	1.3	0.1	1.5	0.7	0.1	-1.0	0.2	0.1	0.2	-0.7	0.8	1.1	5.5	0.8

Figure 4: Scorecard of large-scale indices (winter NAO, AO and AMO) and normalized air temperature anomalies (winter and annual) for five cities between 1980 and 2021. Means and standard deviations for the air temperatures during the 1991–2020 period are provided in the last column (in °C). No means or standard deviations are provided for the large-scale indices (grayed boxes).

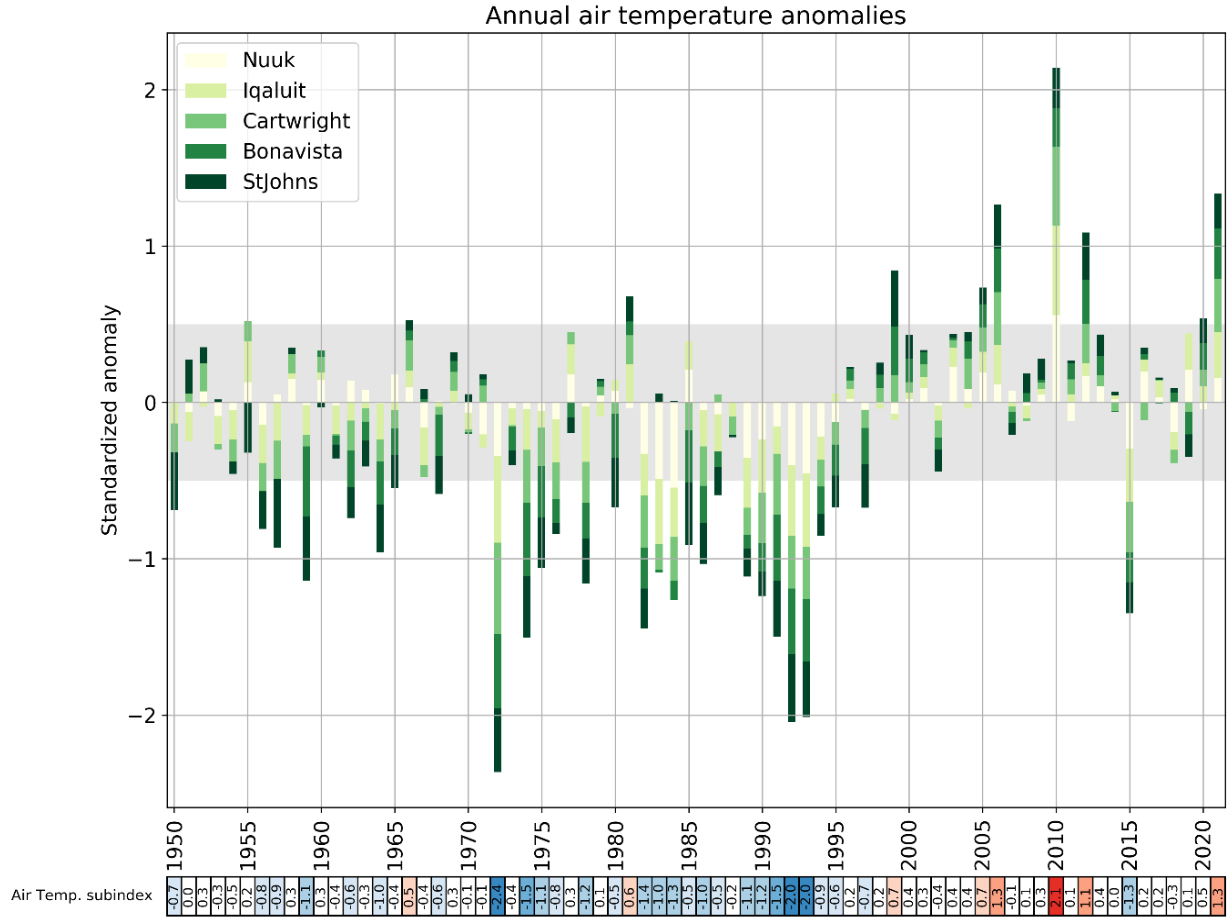

Figure 5: Normalized annual air temperature anomalies for Nuuk, Iqaluit, Cartwright, Bonavista and St. John's. This figure shows the average of the five stations, in which the length of each bar corresponds to the relative contribution of the individual station to the average. The shaded area corresponds to the 1991–2020 average ±0.5 SD, a range considered normal. The numerical values of this time series are reported in a colour-coded scorecard at the bottom of the figure. The bottom scorecard is the average of these five time series, and is used to construct the NL climate index presented in the summary (Figure 40).

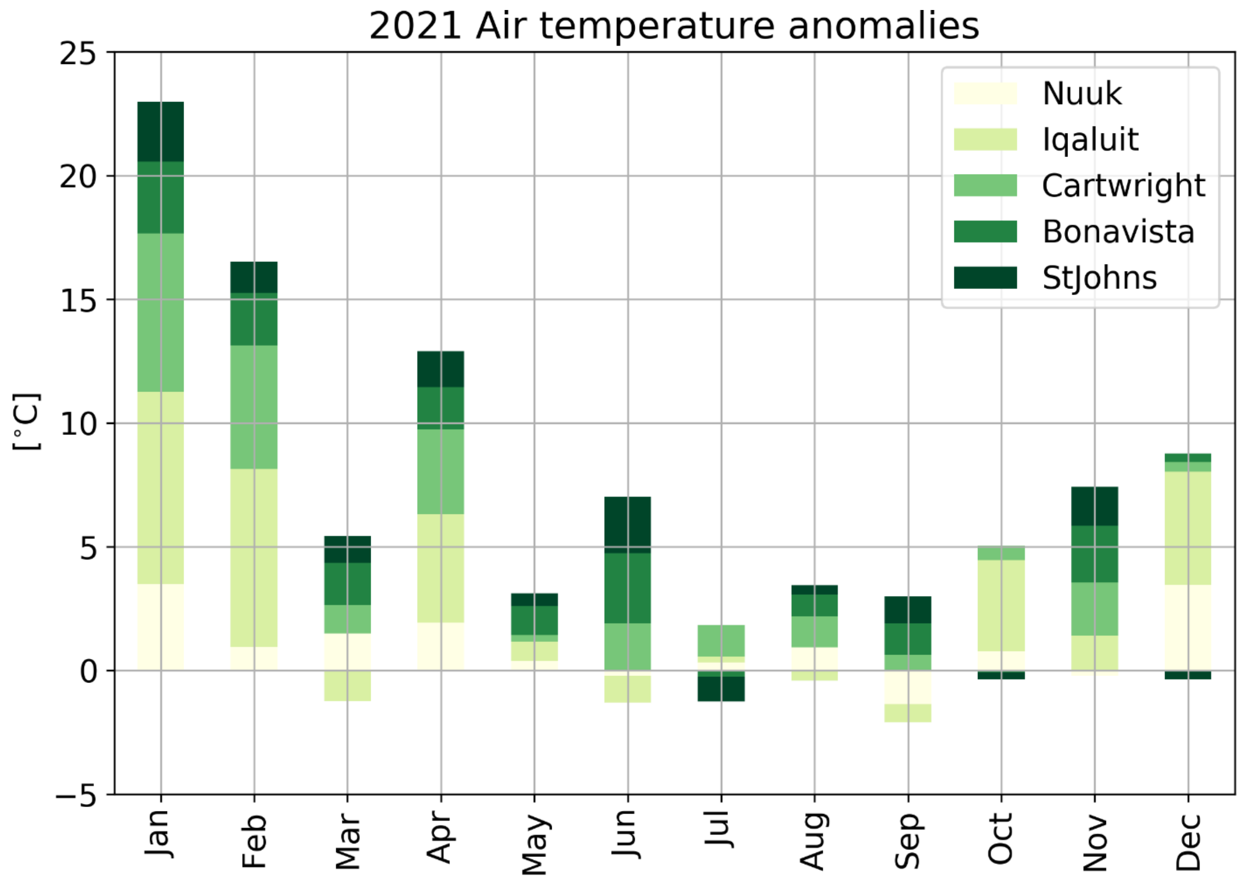

Figure 6: Cumulative monthly air temperature anomalies at Nuuk, Iqaluit, Cartwright, Bonavista and St. John's for 2021.

SEA ICE CONDITONS

Ice cover area, volume and seasonal duration are estimated from ice cover products obtained from the Canadian Ice Service (CIS). These products consist of Geographic Information System (GIS) charts covering the East Coast and Hudson Bay system, the latter providing coverage of the Northern Labrador Shelf. The East Coast region has weekly charts available for 1969–2021 and daily charts for 2009–21 while only weekly charts are available for the Hudson Bay system for 1980–2021. All vector charts were further converted into regular 0.01° latitude by 0.015° longitude grids (approximately 1 km resolution), with ice concentrations and growth stages attributed to each grid point. Average thicknesses (and therefore regional volumes) are estimated from standard thicknesses associated with each stage of ice growth from new ice and nilas (5 cm), grey ice (12.5 cm), grey-white ice (22.5 cm), thin first year ice (50 cm), medium first year ice (95 cm) and thick first year ice (160 cm). Prior to 1983, the CIS reported ice categories with fewer classifications, where a single category of first year ice (≥30 cm) was used with a suggested average thickness of 65 cm. We have found this value leads to underestimates of the seasonal maximum thickness and volume based on high interannual correlations between the estimated volume of the weekly seasonal maximums and its area or sea-ice season duration. The comparisons of the slope of these correlations pre- and post-1983 provided estimates of first-year ice thickness of 85 cm in the Gulf of St. Lawrence and 95 cm on the Newfoundland and Labrador Shelf for this single first year ice category, which were used instead of the suggested 65 cm.

Several products were computed to describe the sea-ice cover inter-annual variability. The day of first and last occurrence, ice season duration (Figure 7) and the distribution of ice thickness during the week of maximum volume (Figure 8) are presented as maps. These two figures combine information from the East Coast sea ice charts and Hudson Bay system charts, leading to a slight jump in the climatology maps of first occurrence and duration. This occurs because there are often missing weeks in the Hudson Bay charts around the period of first occurrence on the northern Labrador Shelf. Therefore anomalies of these two parameters have more uncertainty than the rest. Regional scorecards of anomalies for the first and last day of ice, duration of the sea ice season and maximum ice volume are presented in Figure 9 for the Labrador and Newfoundland shelves. Here, the areas defined as the Northern and Southern Labrador shelves and the Newfoundland Shelf are depicted in Figure 8, with the Newfoundland Shelf and Gulf of St. Lawrence delimited at the Eastern end of the Strait of Belle Isle. Evolution of the ice volume during the 2021 ice season is presented in Figure 10 for the three regions in relation to the climatology and historical extremes. The Northern Labrador Shelf progression is shown using weekly data extracted from Hudson Bay charts, while the others are shown using daily data extracted from East Coast charts. Time series of seasonal maximum ice volume, area (excluding thin new ice) and ice season duration are presented for the Northern (top) and Southern (middle) Labrador Shelf and for the Newfoundland Shelf (bottom) in Figure 11. The December-to-April air temperature anomaly at Cartwright showed the best correlation with sea ice properties and is included with reversed scale in the Newfoundland Shelf panel. The durations shown in Figure 9 and Figure 11 are different products. The first corresponds to the number of weeks where the volume of ice anywhere within the region exceeded 5% of the climatological maximum, while the second is the average duration at every pixel of Figure 7, which is much shorter than the first.

Ice typically starts forming in December along the Labrador coast and only by late February at the southern most extent of sea-ice presence (Figure 7).The last occurrence is usually in late June to early July on the Labrador coast, leading to sea-ice season durations of 23 weeks or more. There has been a declining trend in ice cover severity since the early 1990s, reaching the lowest values in 2010 and 2011, with a rebound in 2014 (Figure 9 and Figure 11). On the Newfoundland Shelf, the sea ice metrics of annual maximum ice area, volume, and ice cover duration are all well-correlated with each other (R^2 = 0.70 to 0.74; Figure 11). The strongest correlation with air temperature was found between the December-April air temperature anomaly at Cartwright and the sea-ice metrics of the Newfoundland Shelf (R^2 = 0.64–0.80), indicative of the advective nature of the Newfoundland Shelf sea ice; i.e. strong ice cover is associated with cold air temperatures in the source area. Sensitivity of the Newfoundland Shelf ice cover to increases in air temperature (e.g. through climate change) can thus be estimated using 1969–2021 co-variations between winter air temperature at Cartwright and sea-ice parameters, which indicate losses of 14 km^3, 26,000 km^2 and eight days of sea-ice season for each 1°C increase in winter air temperature.

In 2021, the sea-ice cover first appeared at a near normal date on the Northern Labrador Shelf and inshore on the Southern Labrador Shelf, later than normal by many weeks offshore and on northern parts of the Newfoundland Shelf, and never appeared at all on southern parts of the Newfoundland Shelf (Figure 7).This lead to regional numbers that were also later than normal (Figure 9). The last occurrence was much earlier than normal everywhere (Figure 7 and Figure 9). Sea ice volumes were below normal throughout the season in the three regions (Figure 10), reaching daily record lows in May to early June, late April to mid-May and mid to late April respectively in the three north-to-south regions. The seasonal maximum ice volumes were below normal in the three regions, at 75 km^3 (-1.0 SD), 59 km^3 (-1.5 SD) and 18 km^3 (-1.3 SD) (Figure 9), while the December-to-June seasonal averages were the second lowest of the time series (after 2011 for the two Labrador Shelf regions and 2010 for the Newfoundland Shelf). The bulk durations (Figure 9) on the Northern Labrador, Southern Labrador and Newfoundland Shelves were below normal, at 165 (-1.1 SD), 129 (-1.8 SD) and 47 days (-2.0 SD), respectively, while the spatial average durations were 91 (-1.9 SD), 57 (-1.8 SD) and 9 days (-1.8 SD), respectively (Figure 7 and Figure 11). An overview of sea ice conditions (volume and season duration) for NL since 1969 is presented in Figure 12 as the average of normalized anomalies. In 2021, this index was below normal at -1.5 SD and third lowest of the time series after 2010 and 2011.

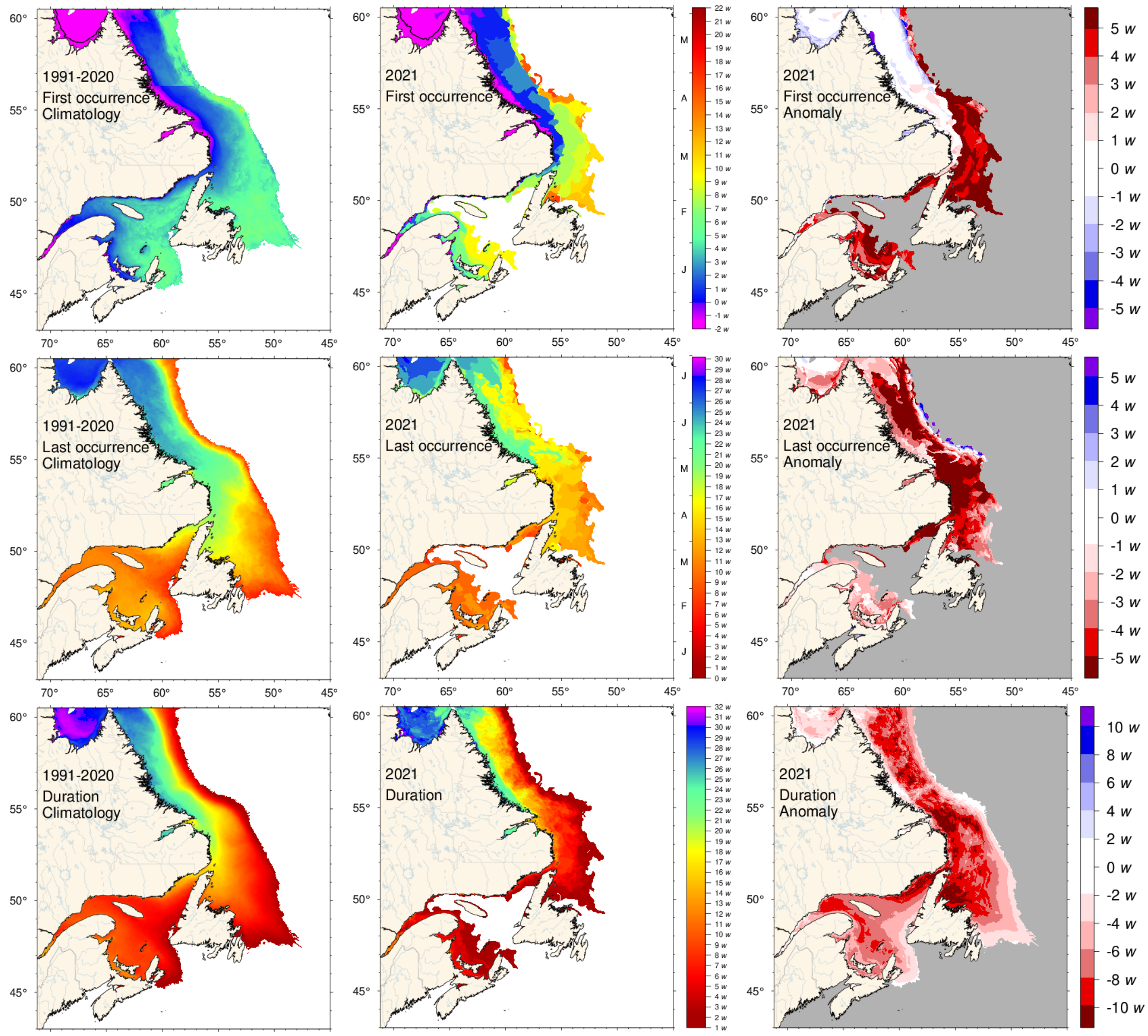

Figure 7: First (top) and last (middle) occurrence of ice and ice season duration (bottom) based on weekly data. The 1991–2020 climatologies are shown (left) as well as the 2021 values (middle) and anomalies (right). First and last occurrences are defined here as the first and last weekly chart in which any amount of ice is recorded for each pixel and are illustrated as day-of-year. Ice duration sums the number of weeks with ice cover for each pixel. Climatologies are shown for pixels that had at least 15 years out of 30 with occurrence of sea-ice, and therefore also show the area with 50% likelihood of having some sea-ice at any time during any given year. The duration anomaly map includes pixels with no ice cover where some was expected based on the climatology.

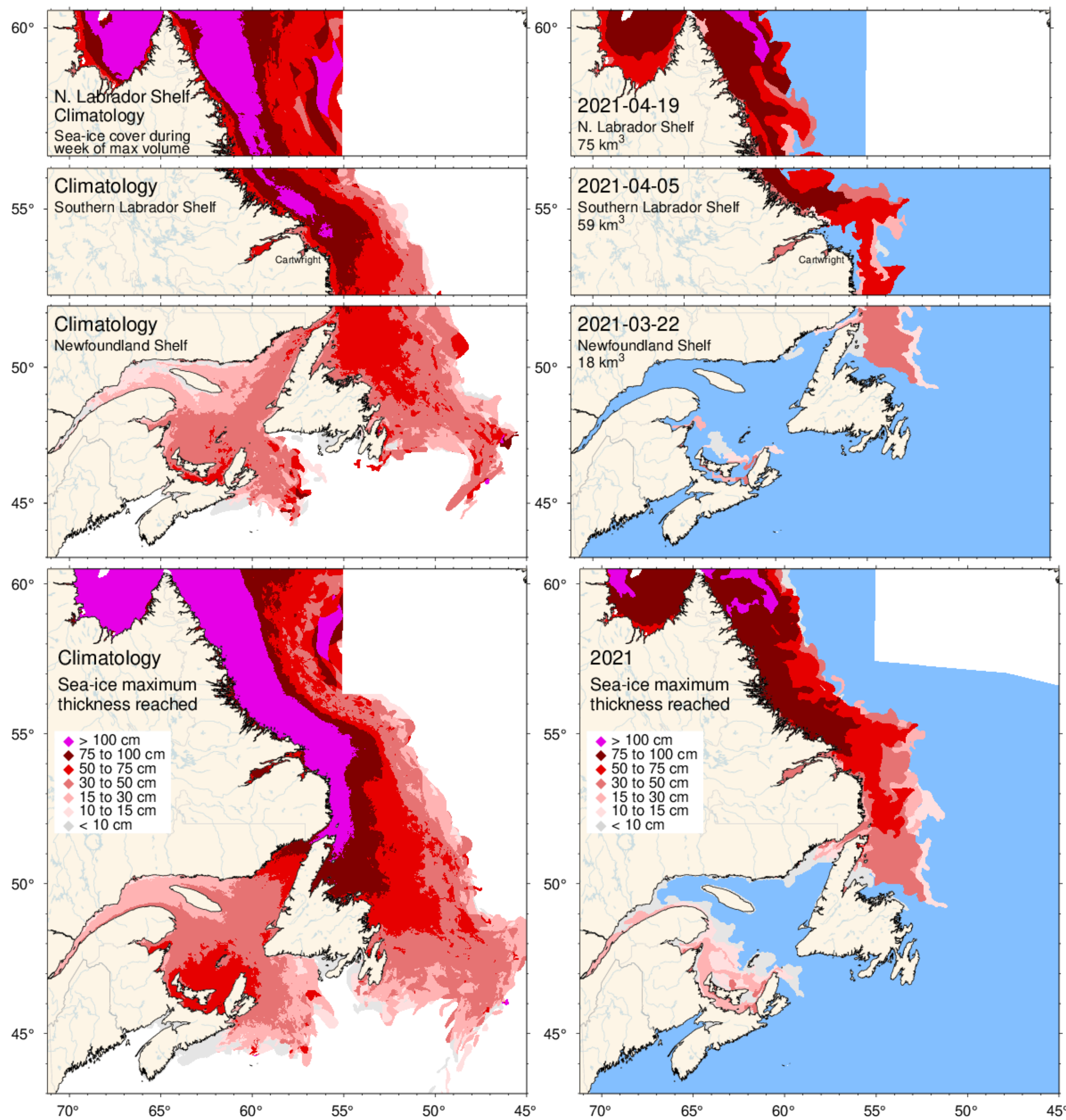

Figure 8: Ice thickness map for 2021 for the week with the maximum annual volume on the Newfoundland and Labrador Shelf (three upper right panels) and similarly for the 1991–2020 climatology of the weekly maximum (three upper left panels). Note that these maps reflect the ice thickness distribution on that week. The maximum ice thickness observed at any given location during the year is presented in the lower panels, showing the 1991–2020 climatology and 2021 distribution of the thickest ice recorded during the season at any location.

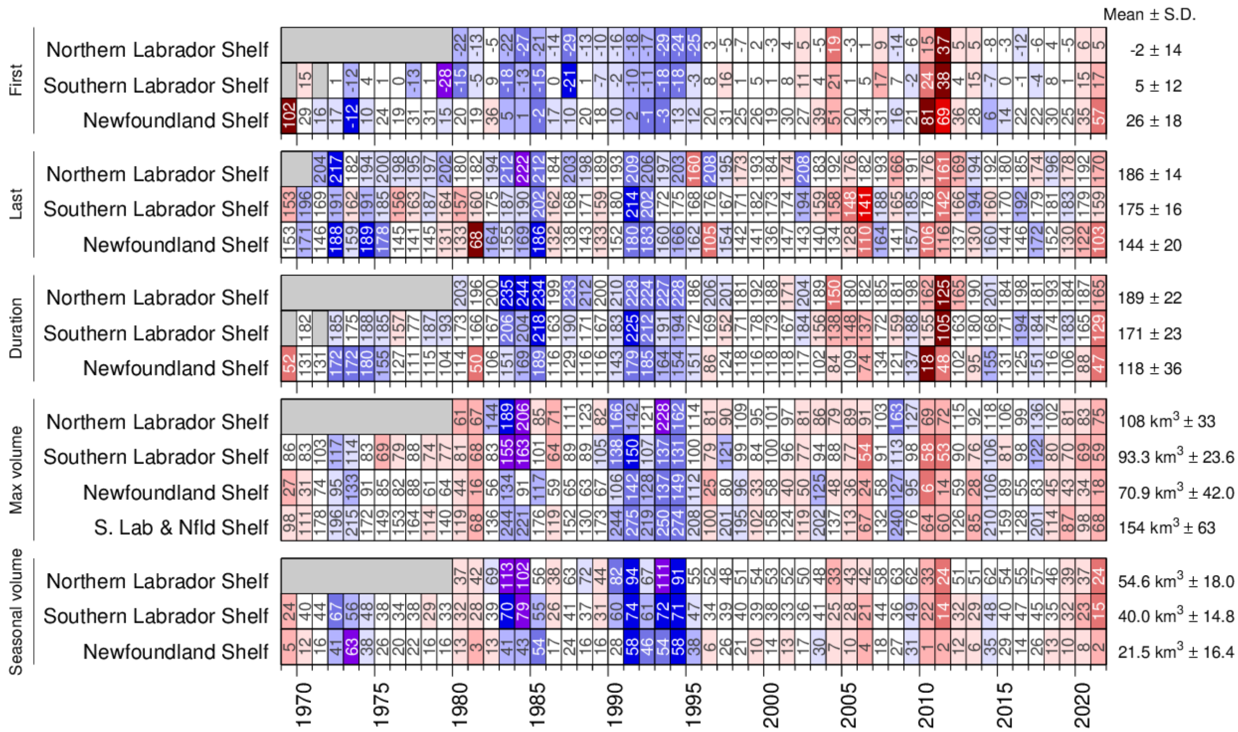

Figure 9: First and last day of ice occurrence, ice duration, maximum seasonal ice volume and average seasonal (DJFMAMJ) ice volume by region. The moment when ice was first and last observed in days from the beginning of each year is indicated for each region, and the color code expresses the anomaly based on the 1991–2020 climatology, with blue (cold) representing earlier first occurrence and later last occurrence. The threshold is 5% of the climatological average of the seasonal maximum ice volume. Numbers in the table are the actual day of the year or volume, but the color coding is according to normalized anomalies based on the climatology of each region. Duration is the numbers of days that the threshold was exceeded. Seasonal average volumes (lowermost scorecard) are reported in the ICES Report on Ocean Climate (e.g. Cyr and Galbraith 2020a).

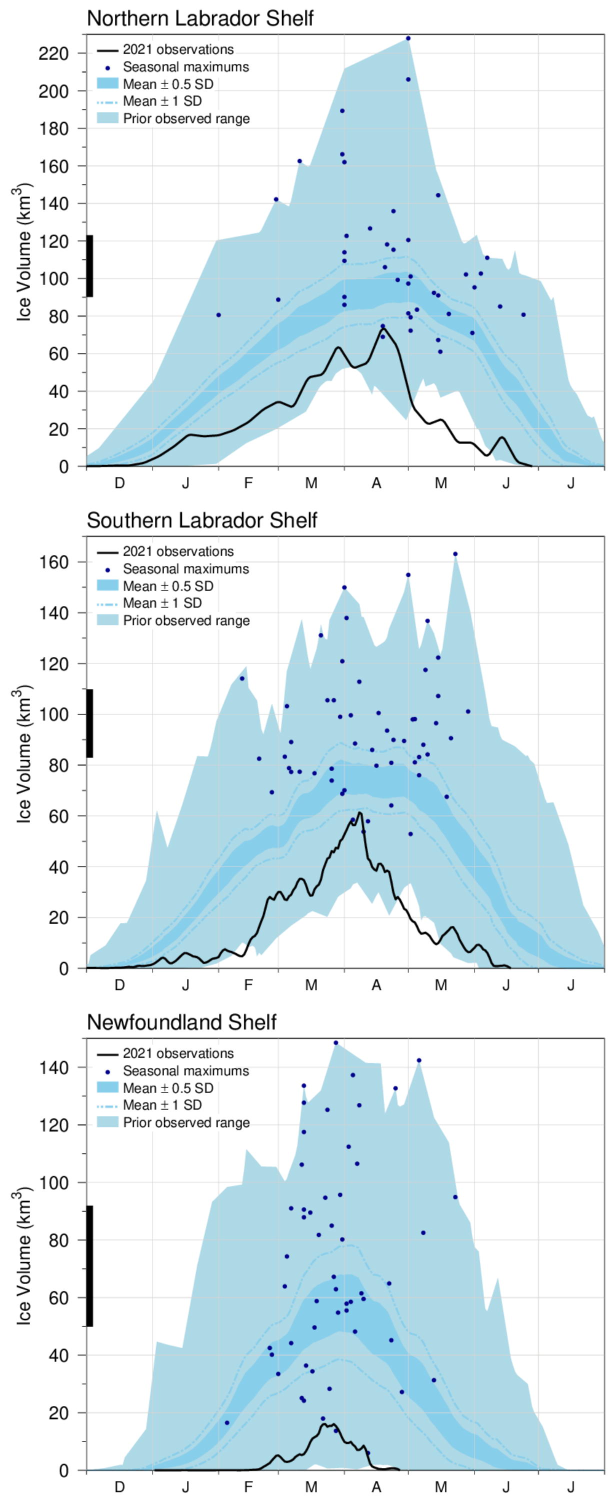

Figure 10: Time series of the 2020–21 mean ice volume (black lines) for the Northern Labrador Shelf (top), Southern Labrador Shelf (middle), and Newfoundland Shelf (bottom), the 1991–2020 climatological mean volume ±0.5 and ±1 SD (dark blue area and dashed line respectively), the minimum and maximum span of 1969–2021 observations (light blue), and the date and volumes of 1969–2021 seasonal maximums (blue dots). The black thick line on the left indicates the mean volume ±0.5 SD of the annual maximum ice volume, which is higher than the peak of the mean daily ice volume distribution.

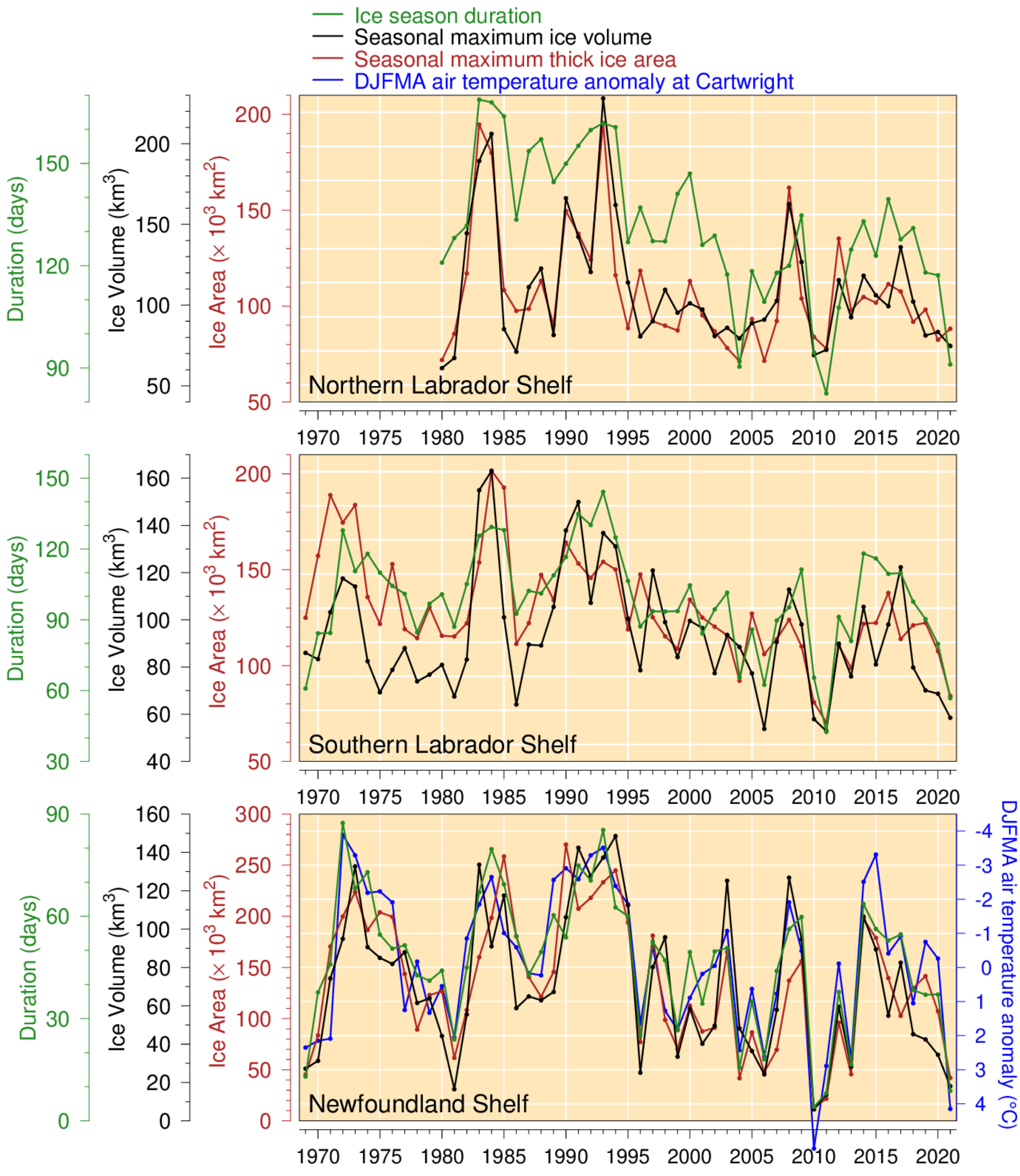

Figure 11: Seasonal maximum ice volume (black lines) and area (excluding ice less than 15 cm thick; red lines), and ice season duration (green lines) for the Northern and Southern Labrador Shelf (top and middle, respectively) and the Newfoundland Shelf (bottom), and December-to-April air temperature anomaly at Cartwright (blue line).

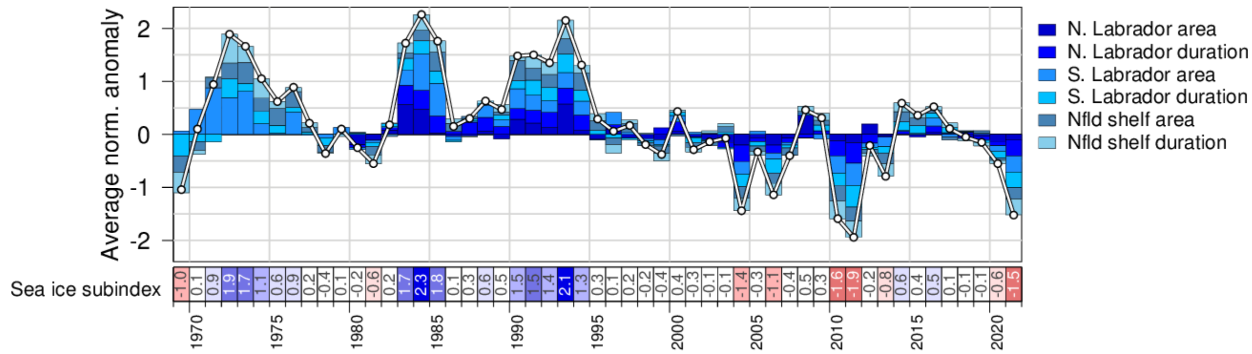

Figure 12: Newfoundland and Labrador sea ice index established by averaging the normalized anomalies of volume and duration of sea ice for Newfoundland and Labrador shelves (black and green time series in Figure 11). This sea ice index contributes to the NL climate index described in the summary (Figure 40).

ICEBERGS

Iceberg counts obtained from the International Ice Patrol of the US Coast Guard indicate that only one iceberg drifted south of 48ºN onto the Northern Grand Bank during 2021, in February (undiscernible from Figure 13 and Figure 14). This number is much lower than the climatological (1991–2020) average of 771. Other years have also seen similarly low numbers. For example, only one iceberg was observed in 2010, two in 2011 and 13 in 2013. Only two years (1966 and 2006) in the 120-year time series have reported no icebergs south of 48ºN. More than 1,500 icebergs have been observed in some years during the cold periods of the early 1980s and 1990s, including the all-time record of 2,202 in 1984, along with a recent high number of 1,515 in 2019. Years with low iceberg numbers on the Grand Banks generally correspond to higher than normal air temperatures, lighter-than-normal sea-ice conditions, and warmer than normal ocean temperatures on the NL Shelf. As such, the normalized anomaly of the number of icebergs (scorecard at the bottom of Figure 13) is used as one component of the NL climate index presented in the summary.

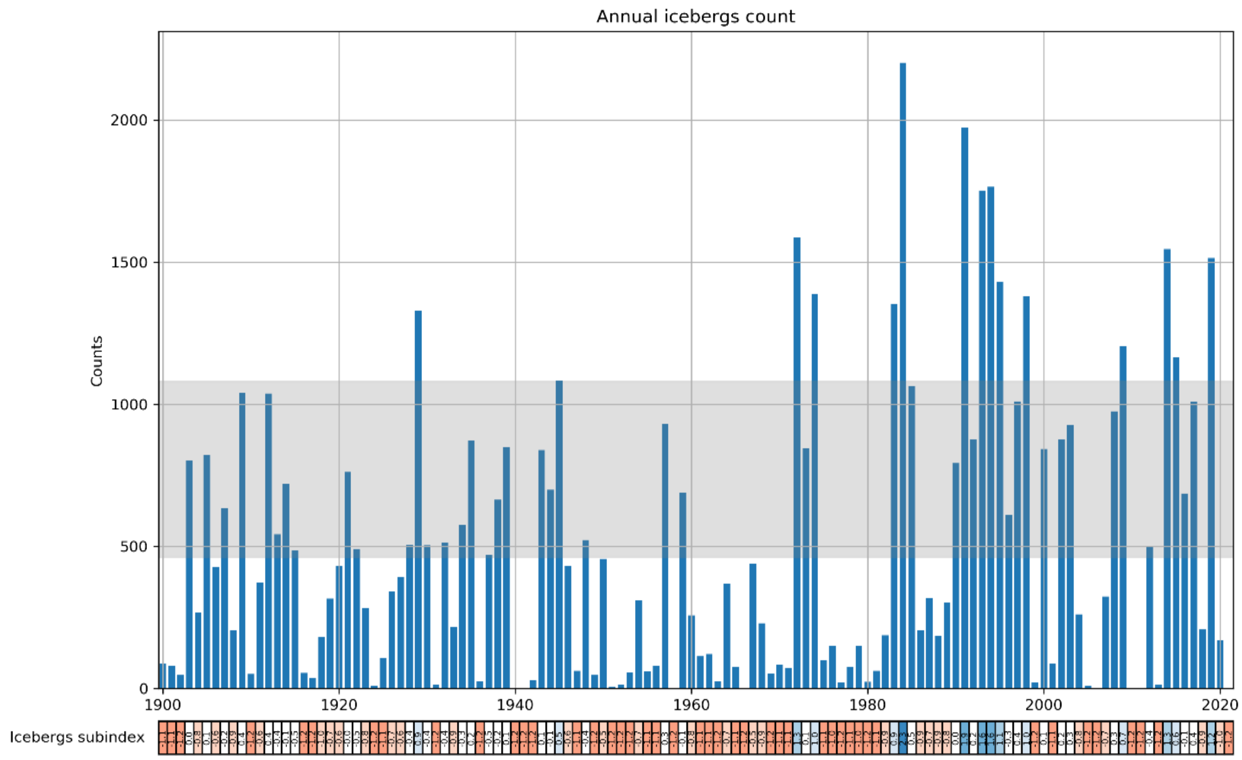

Figure 13: Annual iceberg count crossing south of 48°N on the northern Grand Bank. The shaded area corresponds to the 1991–2020 average ±0.5 SD. The data are from the International Ice Patrol (1995). The normalized anomaly of this time series are color-coded in the bottom scorecard. This iceberg sub-index contributes to the NL climate index described in the summary (Figure 40).

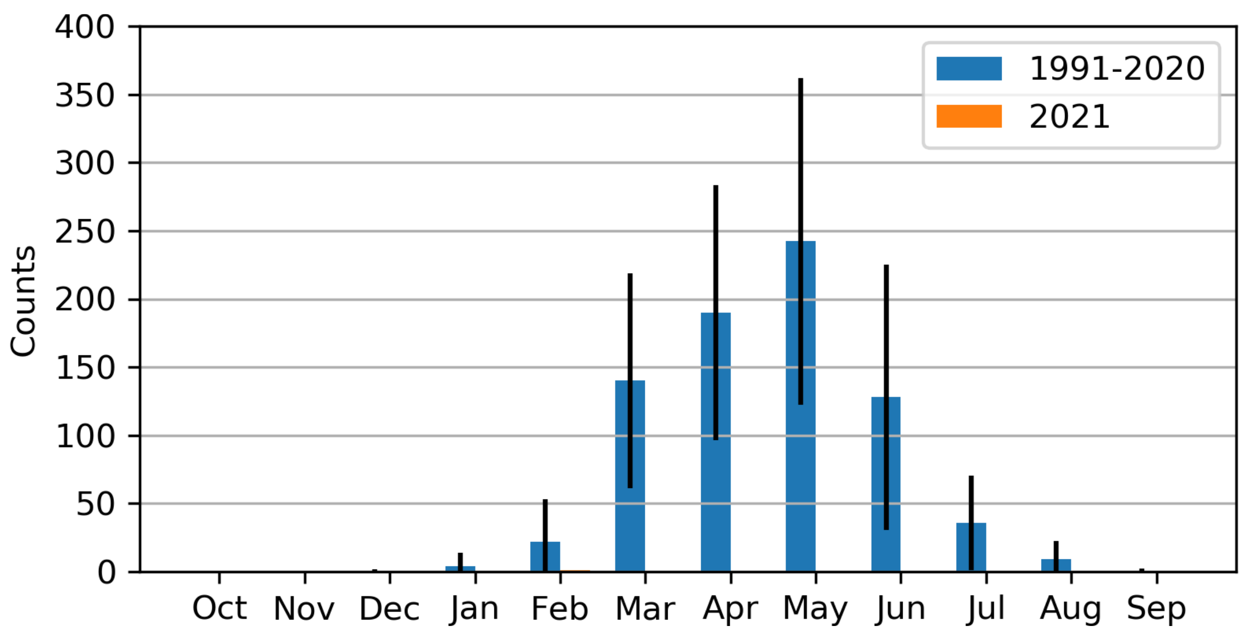

Figure 14: Monthly count of icebergs crossing south of 48°N on the northern Grand Bank during the annual iceberg season (from October to September). The 1991–2020 climatological average is in blue (with the black vertical bars corresponding to ±0.5 SD) and the counts for the year 2021 are in orange. Only one iceberg was detected in February (not visible in this figure). The data are from the International Ice Patrol (1995).

SATELLITE SEA-SURFACE TEMPERATURE

The Sea Surface Temperatures (SSTs) product used here is a blend of data from Pathfinder version 5.3 (1982–2014), the Maurice Lamontagne Institute (1985–2013) and the Bedford Institute of Oceanography (1997–2021). Monthly temperature composites are based on averaged daily anomalies to which monthly climatological average temperatures are added (see Galbraith et al. 2021 for details). Figure 15 shows the weekly evolution of the SSTs (black lines in each panel) for NAFO divisions 2GHJ3KLMNOP cropped at the shelf break (see Figure 1) in relation to the 1991–2020 climatology (blue shades). The color-coded anomalies are shown below each panel as weekly, monthly and seasonal scorecards. Only SST measurements during the ice-free periods of the year are considered. This seasonal windows range from as short as June to September on the northern Labrador Shelf (NAFO division 2H), to as long as March to November in the south coast of Newfoundland (NAFO division 3P).

In 2021, monthly average SSTs were generally normal to above normal in ice-free areas across the zone, with the only negative monthly anomalies being reached in NAFO divisions 3LNO in October (Figure 15, middle scorecards at the bottom of panels). Note that it was especially warm during September in northern Labrador (Div. 2GH) and during October in southern Newfoundland (Div. 3P), with series records for the month and region (since 1981). In terms of seasonal anomalies, while 3LNO were normal, all other divisions were above normal (Figure 15, bottom scorecard in each panel).

SSTs averaged over the ice-free months were normal to above normal across the NL Shelf zone and on average above-normal for the second year in a row, at +0.7 and +0.8 SD in 2020 and 2021, respectively (Figure 16, scorecard at the bottom). Before this, the last occurrence of above normal SSTs across the zone was in 2014. The record-high SST for the NL Shelf was reached in 2012 (+1.5 SD), while the record lows were reached in 1992 and 1991 (-2.0 and -1.9 SD, respectively).

Note that air temperature has been found to be a good proxy of sea surface temperature. The warming trend observed in air temperature since the 1870s of about 1°C per century is also expected to have occurred in surface water temperatures across Atlantic Canada (Galbraith et al. 2021).

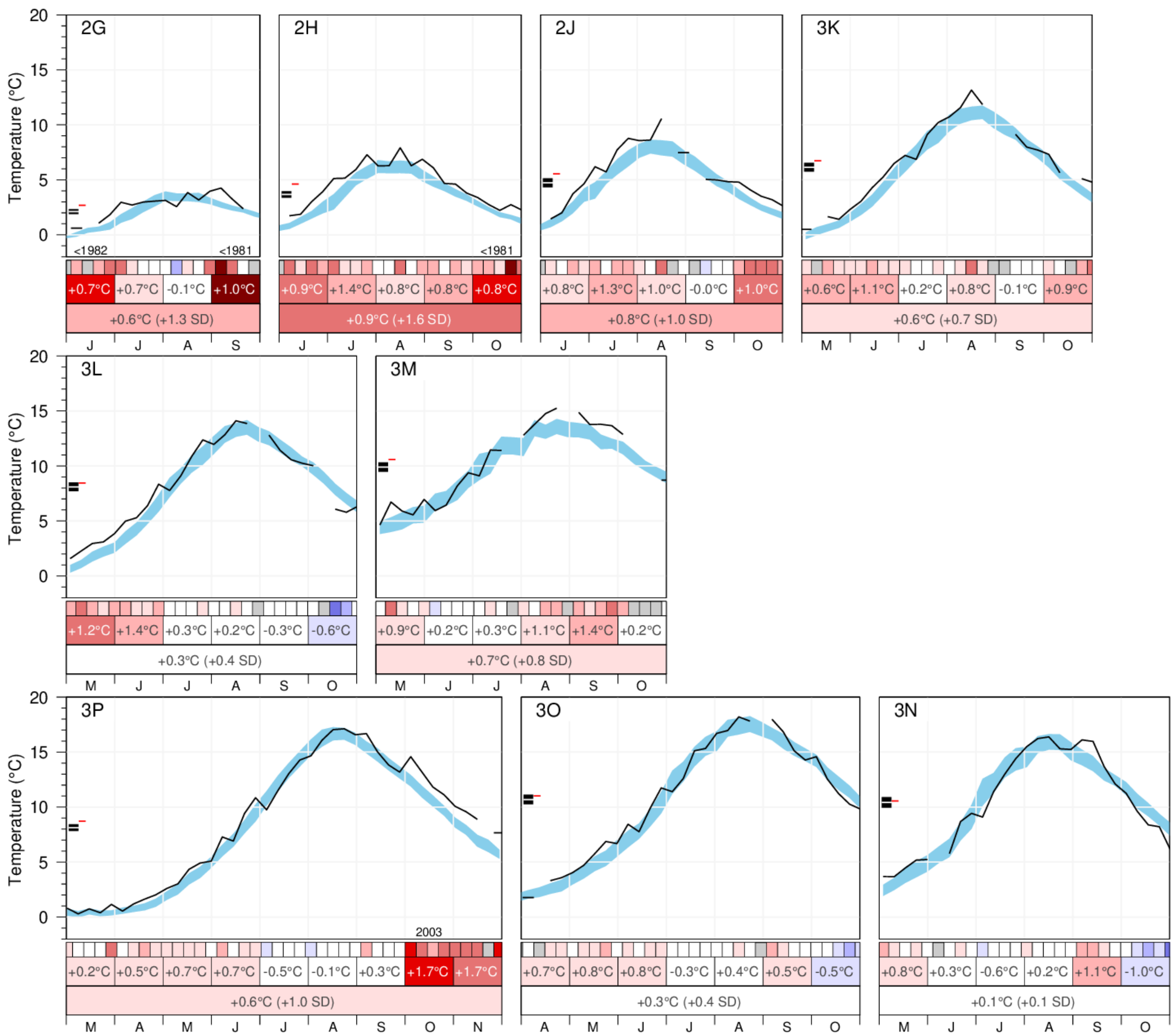

Figure 15: Weekly evolution of AVHRR Sea surface temperature evolution in 2021 for NAFO divisions 2GHJ3KLMNOP (black lines) during the ice-free season (season-length variable). Broken lines indicate that the threshold for the number of good pixel was not reached during these weeks (no data). The blue area represents the 1991–2020 climatological weekly mean ±0.5 SD. Scorecards representing the weekly, monthly and seasonal averages (in °C) appear at the bottom of each panel and are colour-coded according to the normalized anomalies (top, middle and bottom row, respectively). The two black ticks along the y-axis correspond to the seasonal climatological average ±0.5 SD, while the red tick represents the 2021 seasonal average.

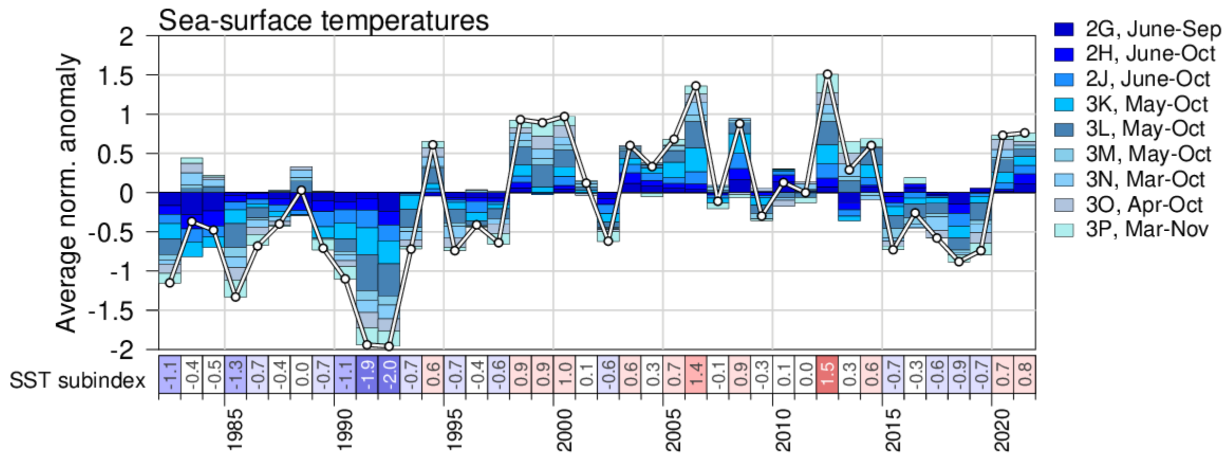

Figure 16: Northwest Atlantic SST index built from the average of the seasonal anomalies for all NAFO divisions (bottom rows of panels in Figure 15). This index contributes to the NL climate index described in the summary (Figure 40).

OCEAN CONDITIONS ON THE NEWFOUNDLAND AND LABRADOR SHELF

The following section presents observations of various ocean parameters (long-term monitoring Station 27, standard hydrographic sections, bottom ocean conditions, etc.).

LONG-TERM OBSERVATIONS AT STATION 27

Station 27 (47°32.8’N, 52°35.2’W), is located in the Avalon Channel off Cape Spear, NL (Figure 1). It is one of longest hydrographic time series in Canada with frequent, near-monthly, occupations since 1948. In 2021, the station was however only occupied 9 times (April 23, June 29, July 19, August 21, September 25, October 6, October 13, November 22, and December 20), including 5 Conductivity-Temperature-Depth (CTD)-only casts, 4 full AZMP physical-biogeochemical sampling and 0 Expandable Bathythermograph (XBT). Since the first observation was only made late April, 2021 is perpetuating a recurrent problem since 2016 of late first occupation of the year. These late starts miss the re-stratification of the water column that occur early April, which can be used to predict the timing of the phytoplankton bloom in the area.

Since 2017, an automatic profiling system installed on a surface buoy (type Viking) usually provides extended temporal coverage of temperature (T) and salinity (S) at Station 27. Unfortunately, in 2021, the system was deployed in late April and stopped functioning early June. The buoy was recovered and re-deployed late in the summer, but the CTD data suffered electronic spikes that have not been corrected at the time this report was written.

Station occupation and April-June Viking buoy automatic casts were combined to obtain the annual evolution of temperature and salinity at Station 27, as well as the anomaly compared to the 1991–2020 climatology, shown in Figure 17 and Figure 18. These figures demonstrate the seasonal warming of the top layer (~20 m), with temperature peaking in August before being mixed during the fall. The CIL; (Petrie et al. 1988), a remnant of the previous winter cold layer and defined as temperature below 0°C (thick black line in Figure 17) is also evident below 100 m throughout the summer. Interestingly, the coldest water body within the CIL (darkest shades of blue in the middle panel of Figure 17) is generally found in the summer between mid-June and mid-August, suggesting advection of cold waters from the Labrador Shelf and the Arctic to the Newfoundland Shelf. The surface layer is generally freshest between early-September and mid-October, with salinities below 31 (Figure 18). These low near-surface salinities, generally from early summer to late fall, are a prominent feature of the salinity cycle on the Newfoundland Shelf and is largely due to the melting of coastal sea-ice. This presence of large volume of freshwater late in the summer season also points out towards advection from northern areas (Labrador and the Arctic).

The rapid cooling observed above the CIL in October 2021 (which looks like near-vertical contours in Figure 17, top panel) is the result of a storm that hit St. John's on October 8-9, in between the two occupations of October 6 and October 13. The storm caused a rapid mixing of the water column and a deepening of the CIL. This led to cooling of the upper part of the water column and a warming at depth (see the rapid vertical displacement down of the September-October warm anomaly in Figure 17, bottom panel). This is also accompanied by a similar displacement of the fresh anomaly (Figure 18, bottom panel).

Overall, however, most of the water column was warmer and fresher than normal in 2021 (Figure 17 and Figure 18, top and bottom panels). Over 2021, the annual temperature anomaly (defined as the average of monthly anomalies) for the vertically averaged (0–176 m) temperature was at a record-high since 1951 (Figure 19, top panel). Note that while the fact that Station 27 was les sampled in 2021 compared to historical data adds an extra source of uncertainty on this record, the fact that the warm anomaly is consistent across the year (Figure 18) adds confidence to this result. In addition, warm temperatures at Station 27 are also expected during mild winters such as the one observed in 2021 (see sections on air temperature and sea ice).

The annual anomaly for the vertically-averaged salinity was its second-freshest since 1971 (the freshest was 2018). The fresh anomaly of the early 1970s (Figure 19, bottom panel) is commonly referred to as the Great Salinity Anomaly in the North Atlantic (Dickson et al. 1988). Normalized anomalies of temperature and salinity for all years since 1980 and for different depth ranges (0–176 m, 0–50 m and 150–176 m) are reported in scorecards in Figure 20.

The summer (May-July) CIL statistics at Station 27 since 1951 are presented in Figure 21. Here the CIL mean temperature corresponds to the average of all temperature below 0°C. The CIL thickness as well as the CIL core temperature (the minimum temperature of the CIL) and its depth are also presented in Figure 21. The striking feature in this figure is the exceptionally warm anomaly from the early 1960s to the mid-1970s for the CIL mean and core temperatures (coldest temperature within the CIL), top and middle panels, respectively. These warm anomalies are accentuated by the fact that the climatological reference period (1991–2020) includes a relatively cold period that spanned the mid-1980s to the mid-1990s (see Figure 19). After the prevalence of a warm CIL in the early 2010s (with some of the warmest years since the mid-1970s), there has been a cooler period between about 2014 and 2017. In recent years, the CIL was warmer than normal in 2018, 2019 and 2021, while 2020 was in the normal range. The SD of these metrics are reported in a scorecard in Figure 20.

The monthly mean mixed layer depth (MLD) at Station 27 was also estimated from the density profiles as the depth of maximum buoyancy frequency (N) calculated from the monthly averaged density profiles (ρ[z]):

$$N^2 = \frac{-g}{\rho_0} \frac{\Delta\rho(z)}{\Delta z};$$

with g = 9.8 ms^{-2} as the gravitational acceleration, z the depth and ρ_0 the mean density. Here N^2 is calculated using the Gibbs-SeaWater (GSW) Oceanographic Toolbox (McDougall and Barker 2011).

Climatological monthly MLD values, as well as monthly MLDs during 2021, are presented in Figure 22. The climatological annual cycle shows a gradual decrease of the MLD between late fall and summer (mixed layer thickest in December-January and shallowest in July-August). Because of the relatively low number of occupation realized in 2021 (most of the time just one profile per month), it is difficult to confidently draw conclusions related to the MLD. Overall, the MLD was close to normal, except slightly shallow in April, slightly thicker in the summer and much thicker than normal in December. Figure 23 shows a time series of the annual mean values of the MLD (solid gray line) and its 5-year moving average (dashed-black line). In general, there is a strong interannual and decadal oscillation in MLD, with a recent increase since the mid-2000s. A scorecard of annual and seasonal MLD anomalies since 1980 can be found in Figure 20.

Stratification is an important characteristic of the water column since it influences, for example, the transfer of solar heat to lower layers and the vertical exchange of biogeochemical tracers between the deeper layers and the surface. The seasonal development of stratification is also an important process influencing the formation and evolution of the CIL on the shelf regions of Atlantic Canada. It essentially insulates the lower water column from the upper layers, thus slowing vertical heat flux from the seasonally heated surface layer.

The stratification index at Station 27 is computed from the density (ρ) difference between 8 and 50 m for each monthly average density profiles (i.e. $\Delta\rho/\Delta z$). The annual anomalies are then calculated as the average of monthly anomalies. The 2021 and climatological evolution of the stratification throughout the year are shown in Figure 24. The stratification is generally weakest between December and April, before rapidly increasing at the onset of spring until it peaks in August. While the stratification was close to normal or slightly below/above normal for most of 2021, a notable observation is the high stratification in August, followed by a rapid reduction of the stratification in September (Figure 24). This rapid de-stratification is likely a consequence of Hurricane Larry that hit Newfoundland between September 10 and 11 with wind gusts observed at 145 km/h at St. John’s airport.

The interannual evolution of the stratification anomaly since 1950 is shown in Figure 25. While strong decadal variations exists, the main observation is an increase in stratification from the 1950s to about 2000, followed by a slight decrease since. In 2021, the annual stratification was weaker than normal. A scorecard of annual and seasonal stratification anomalies since 1980 can be found in Figure 20.

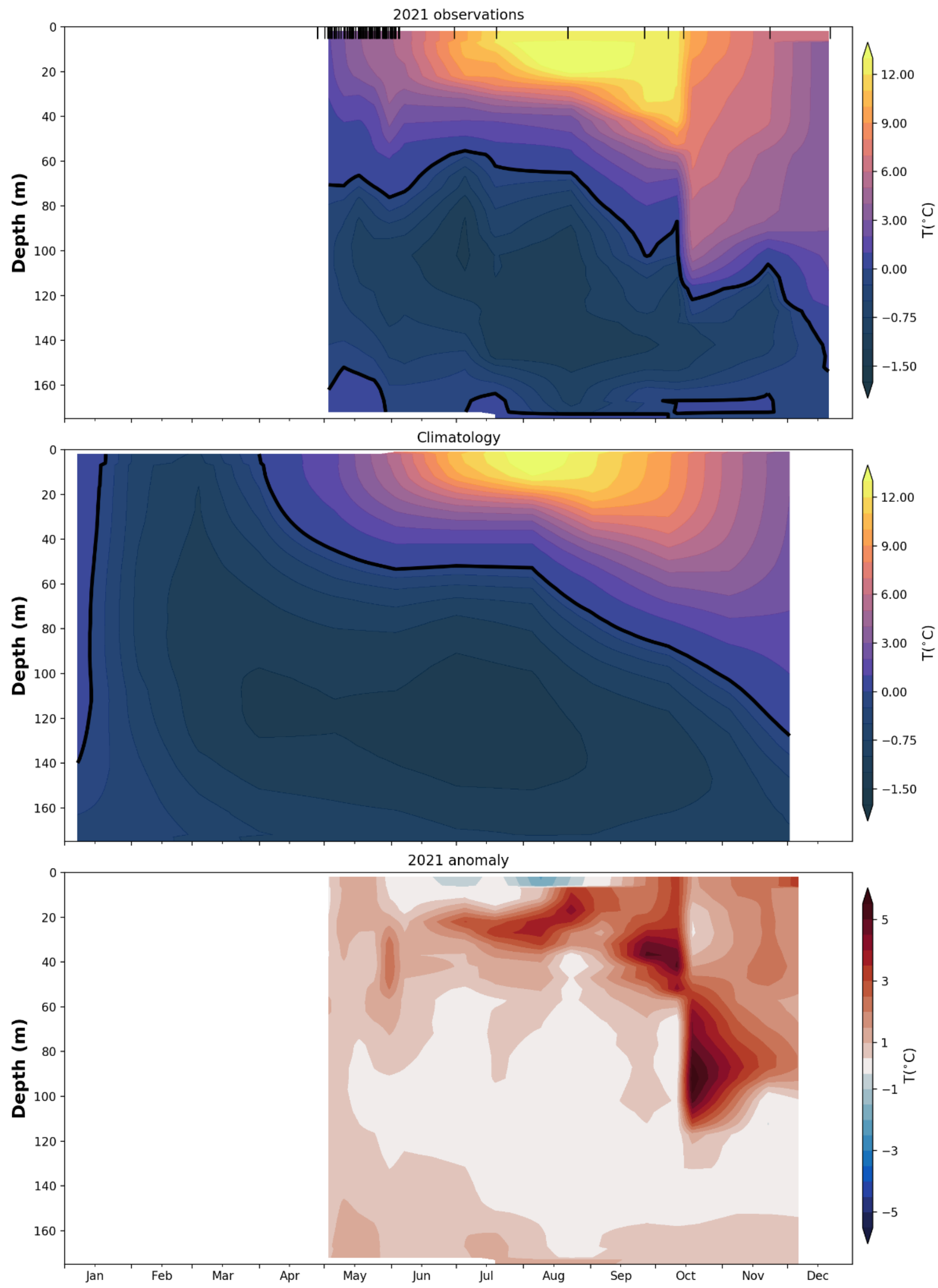

Figure 17: Annual evolution of temperature at Station 27. The 2021 contour plot (top panel) is generated from weekly averaged profiles from all available data, including station occupations and Viking buoy casts (indicated by black tick marks on top of panel). The solid black contour delineates the cold intermediate layer (CIL), defined as water below 0°C. The 1991–2020 weekly climatology is plotted in the middle panel. Note the uneven colorbar used in the two first panels: below 0°C, 0.25°C increments are used, while 1°C increments are used above 0°C. The anomaly (bottom panel) is the difference between the 2021 field and the climatology.

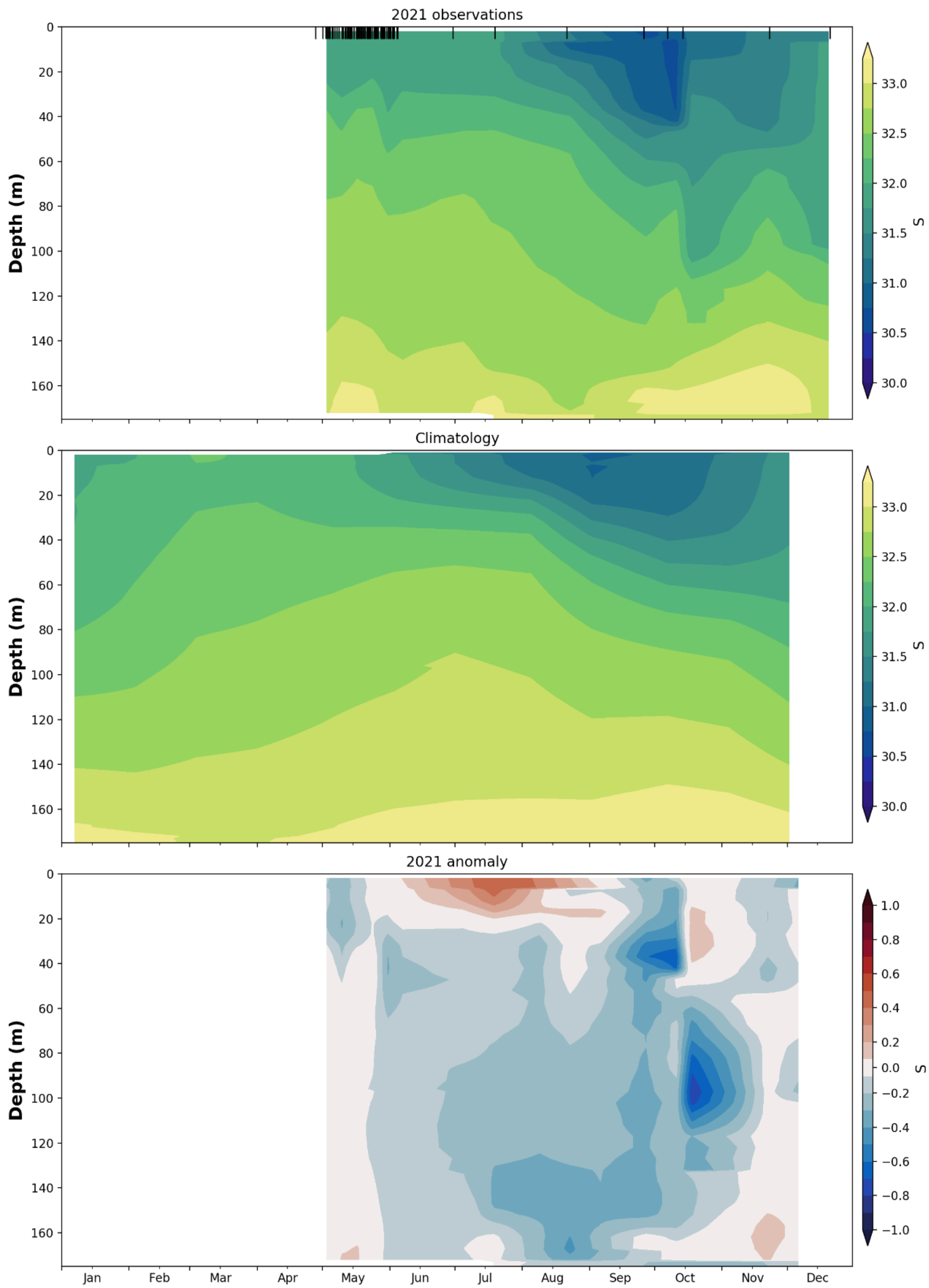

Figure 18: Same as in Figure 17, but for salinity.

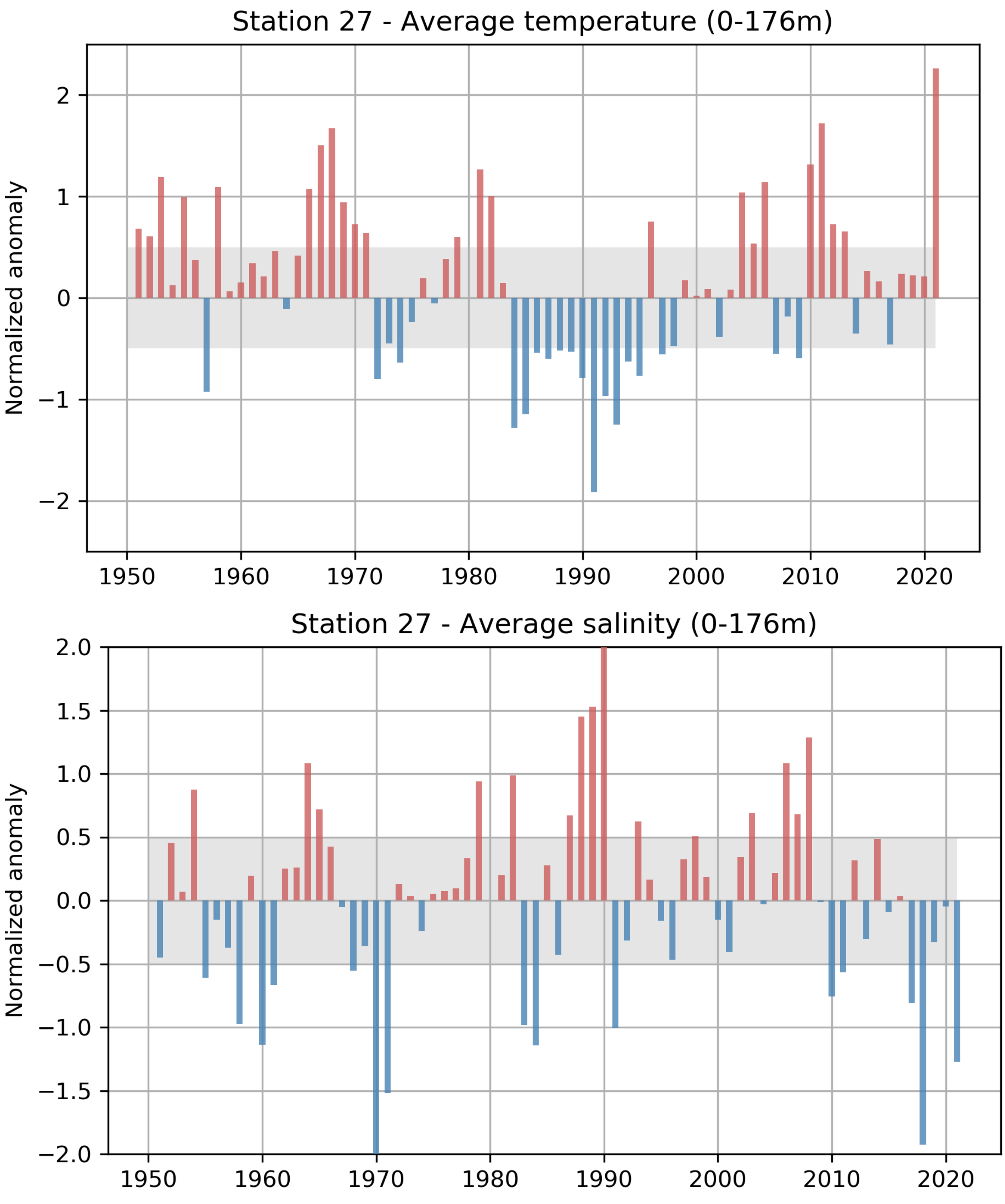

Figure 19: Annual normalized anomaly of vertically averaged (0–176 m) temperature (top) and salinity (bottom) at Station 27 calculated from all occupations since 1951. Only years where at least 8 months of the year are sampled are presented. Shaded gray areas represent the climatological (1991–2020) average ±0.5 SD range considered "normal". These two time series contribute to the NL climate index described in the summary (Figure 40).

	81	82	83	84	85	86	87	88	89	90	91	92	93	94	95	96	97	98	99	00
-- Vertically averaged temperature --																				
Temp 0-176m	1.3	1.0	0.1	-1.3	-1.1	-0.5	-0.6	-0.5	-0.5	-0.8	-1.9	-1.0	-1.2	-0.6	-0.8	0.8	-0.6	-0.5	0.2	0.0
Temp 0-50m	0.8	0.0	0.0	-1.3	-1.1	-0.5	-0.6	-0.6	-0.7	-0.7	-1.6	-0.8	-1.0	-0.3	-0.6	0.4	-0.6	-0.1	0.3	0.1
Temp 150-176m	0.0	-0.6	-0.5	-1.0	-1.5	-0.6	-0.6	-0.5	-0.7	-1.1	-1.4	-1.1	-1.4	-1.2	-0.8	0.2	-0.2	0.1	0.3	0.1
-- Vertically averaged salinity --																				
Sal 0-176m	0.2	1.0	-1.0	-1.1	0.3	-0.4	0.7	1.4	1.5	2.4	-1.0	-0.3	0.6	0.2	-0.2	-0.5	0.3	0.5	0.2	-0.2
Sal 0-50m	0.4	1.7	-0.9	-1.4	0.6	0.6	1.0	1.3	1.9	1.9	-1.3	-0.2	0.2	0.0	-0.9	-0.1	0.0	-0.1	0.0	-0.5
Sal 150-176m	0.5	1.2	0.2	0.5	0.0	-0.6	0.9	2.0	1.0	2.7	-0.6	-0.5	0.8	0.0	0.2	-0.6	0.3	0.7	0.2	0.3
-- Cold intermediate layer (CIL) properties --																				
CIL temp	1.0	0.4	-0.8	-0.8	-1.4	-0.8	-0.5	-0.2	-0.3	0.0	-1.5	-1.1	-1.5	-1.0	-1.0	1.1	-0.6	-0.8	0.2	0.6
CIL core T	0.9	0.0	-0.8	-0.8	-1.4	-1.1	-0.8	0.0	-0.3	-0.3	-1.5	-0.8	-1.2	-1.4	-1.1	1.2	-0.4	-0.7	0.0	0.6
CIL core depth	-3.0	-1.4	1.9	-1.1	1.9	-0.7	0.6	0.0	1.2	2.9	-1.4	0.6	0.9	-0.1	-0.1	1.5	-1.4	-0.7	0.9	1.2
CIL thickness	-1.1	-4.5	-0.1	0.7	0.6	0.1	-0.4	0.3	-1.2	-0.8	2.0	-0.2	0.0	1.0	0.3	-1.3	0.7	0.9	0.1	-0.1
-- Mixed layer depth (MLD) --																				
MLD winter	-0.8	-0.3		0.1	-1.1	-0.6	-0.2		-0.4	0.7	1.2		-0.6	0.6	-1.0	0.3	0.0	0.5	-0.3	0.0
MLD spring	0.4	-0.9	-0.8	-1.7	-1.4	-0.7	-1.0	-0.7	-0.8	-0.1	0.1	-0.5	-0.3	0.6	-0.8	-0.4	-0.6	-0.6	-0.9	0.2
MLD summer	0.7	0.4	-0.3	-0.7	0.1	0.1	-0.6	-0.9	-1.3	-0.4	-0.6	1.4	1.2	0.6	0.7	1.0	0.4	-0.4	-0.3	-0.5
MLD fall			-0.2	-1.2	0.2	0.6	-0.7	-1.0	-0.4	-1.5	-0.2	0.8	-0.7	-0.6	-0.2	-0.7	-0.2	0.3	0.4	0.0
MLD annual	0.2	-0.4	-0.4	-1.1	-0.6	-0.2	-0.7	-0.8	-0.7	-0.4	-0.1	0.6	-0.1	0.3	-0.2	0.1	-0.1	-0.1	-0.3	-0.1
-- Stratification --																				
strat winter		-0.3		-0.1	0.7	-0.3	-0.6		-0.3	-1.0	-1.2		1.5	-1.4	1.5	-0.2	0.5	-0.8	0.4	0.2
strat spring	0.8	-0.1	2.6	1.6	-0.9	-0.2	2.4	0.5	-0.3	-1.1	0.4	-0.4	0.4	-0.5	2.2	-0.5	0.2	0.9	1.1	-0.1
strat summer	1.4	-1.4	-0.1	1.1	-0.1	-0.8	-1.2	0.0	-0.8	-0.4	-0.5	-0.5	-0.7	1.1	0.5	-1.4	-0.1	0.8	1.0	-0.1
strat fall			-1.0	0.2	-0.9	-1.3	-0.5	0.3	-0.1	0.3	1.8	-0.5	-0.6	0.0	0.6	-0.1	0.1	0.4	-0.2	0.6
strat annual	0.9	-0.6	0.3	0.9	-0.2	-0.6	0.2	0.3	-0.3	-0.6	0.5	-0.4	0.2	-0.1	1.1	-0.6	0.1	0.4	0.6	0.2

	01	02	03	04	05	06	07	08	09	10	11	12	13	14	15	16	17	18	19	20	21	$\bar{x}$	sd
-- Vertically averaged temperature --																							
Temp 0-176m	0.1	-0.4	0.1	1.0	0.5	1.1	-0.6	-0.2	-0.6	1.3	1.7	0.7	0.7	-0.4	0.3	0.2	-0.5	0.2	0.2	0.2	2.3	0.6	0.5
Temp 0-50m	0.2	-0.6	0.1	0.6	0.5	1.2	-0.6	0.5	-0.9	0.9	1.1	0.9	0.7	-0.1	0.1	0.5	-0.4	-0.2	-0.4	0.1	1.7	3.5	0.8
Temp 150-176m	0.3	-0.2	-0.3	1.3	0.9	1.0	0.1	-0.2	-0.6	1.1	2.5	0.4	0.6	-0.7	-0.7	-0.6	-0.7	0.5	0.2	1.0	1.9	-0.8	0.4
-- Vertically averaged salinity --																							
Sal 0-176m	-0.4	0.3	0.7	0.0	0.2	1.1	0.7	1.3	0.0	-0.8	-0.6	0.3	-0.3	0.5	-0.1	0.0	-0.8	-1.9	-0.3	0.0	-1.3	32.4	0.1
Sal 0-50m	-0.6	1.0	1.2	0.4	0.4	0.6	0.4	0.7	0.4	-0.9	-0.4	0.3	0.0	0.1	0.0	0.2	-1.0	-0.8	0.7	0.0	-0.5	31.8	0.1
Sal 150-176m	0.0	0.0	-0.5	0.1	0.3	1.3	0.7	0.9	-0.4	0.1	0.0	0.4	-0.6	0.4	-0.3	-0.6	-0.6	-1.7	-1.1	0.5	-1.1	33.0	0.1
-- Cold intermediate layer (CIL) properties --																							
CIL temp	0.5	-0.5	-0.3	1.1	0.1	1.1	-0.6	-0.4	-1.1	2.2	2.1	-0.1	1.0	-0.3	-0.5	-0.1	-0.8	1.3	0.9	-0.1	1.5	-1.0	0.2
CIL core T	0.5	-0.4	-0.4	1.0	-0.1	1.5	-0.5	-0.5	-1.3	2.5	2.0	-0.3	1.3	-0.1	-0.2	-0.3	-0.3	0.7	0.6	-0.2	1.7	-1.4	0.2
CIL core depth	-0.7	1.2	-0.1	-0.1	-0.7	-0.7	-1.4	-1.4	0.9	0.6	-1.4	-1.1	-0.7	2.2	0.6	0.9	0.0	0.2	0.9	-0.7	-1.4	123.2	15.4
CIL thickness	0.2	0.4	-1.3	0.0	0.8	-0.2	1.1	0.9	0.9	-2.4	-1.7	-1.4	0.1	0.5	-0.1	-0.4	1.0	-1.6	-0.6	0.3	-1.5	124.3	11.3
-- Mixed layer depth (MLD) --																							
MLD winter	-0.8	0.2	-0.3	0.7	0.3	1.1	0.1	-0.6	-1.8	-1.2	0.1	-0.3	1.9	0.3	0.8	-0.4			-1.1			59.5	7.8
MLD spring	0.1	0.1	-0.4	-0.2	-0.4	-0.1	0.4	0.0	-0.4	0.1	-0.4	1.3	0.3	0.5	0.0	-0.5	0.2	0.7	1.8		-0.2	37.1	9.0
MLD summer	0.4	-0.5	-0.2	-0.7	-0.6	0.3	-0.7	-0.7	-0.3	-0.4	1.6	-1.0	-0.1	-0.9	0.5	0.9	-0.5	0.3	-0.5	-0.6	1.3	21.8	6.1
MLD fall	-0.6	0.2	-0.6	0.6	0.5	-0.6	0.3	-0.4	1.0	-0.5	0.5	1.1	-0.5	0.4	0.7	-0.9	-0.7	0.3	0.5	0.0	0.8	57.1	7.3
MLD annual	-0.2	0.0	-0.4	0.1	-0.1	0.1	0.0	-0.4	-0.2	-0.4	0.4	0.3	0.1	0.0	0.5	-0.2	-0.3	0.4	0.4	-0.3	0.6	43.9	17.4
-- Stratification --																							
strat winter	0.2	0.5	0.4	-0.3	-0.5	0.0	-0.5	1.0	0.7	0.2	0.1	-0.8	-1.1	-1.0	0.0	-0.6			-0.1			0.008	0.001
strat spring	0.2	-0.8	-0.7	0.1	0.2	0.6	0.1	-0.2	1.1	-0.3	-0.1	0.0	-0.3	-0.8	0.0	-0.4	0.3	-1.1	-1.1		0.8	0.017	0.009
strat summer	0.4	0.1	-0.6	-0.2	0.3	0.0	0.9	0.1	0.3	-0.5	-1.9	0.0	0.9	1.9	-1.2	-0.5	1.5	-1.2	-1.0	0.5	-0.4	0.059	0.01
strat fall	1.1	-0.9	0.3	0.0	-0.5	0.8	-0.2	0.8	-1.1	0.6	-0.8	-0.8	0.0	-0.4	-1.0	1.3	0.3	-0.6	-0.9	0.3	-1.0	0.018	0.011
strat annual	0.4	-0.4	-0.2	-0.1	-0.1	0.4	0.1	0.4	0.1	0.0	-0.7	-0.4	0.0	0.1	-0.6	0.0	0.7	-1.0	-0.9	0.4	-0.1	0.025	0.022

Figure 20: Annual normalized anomalies of hydrographic parameters for Station 27. The different boxes from top to bottom are: vertically averaged temperature and salinity for different depth ranges, cold intermediate layer (CIL) properties, mixed layer depth (MLD), and stratification for the 4 seasons and annual average. The cells are color-coded according to Figure 2. Gray cells indicate an absence of data.

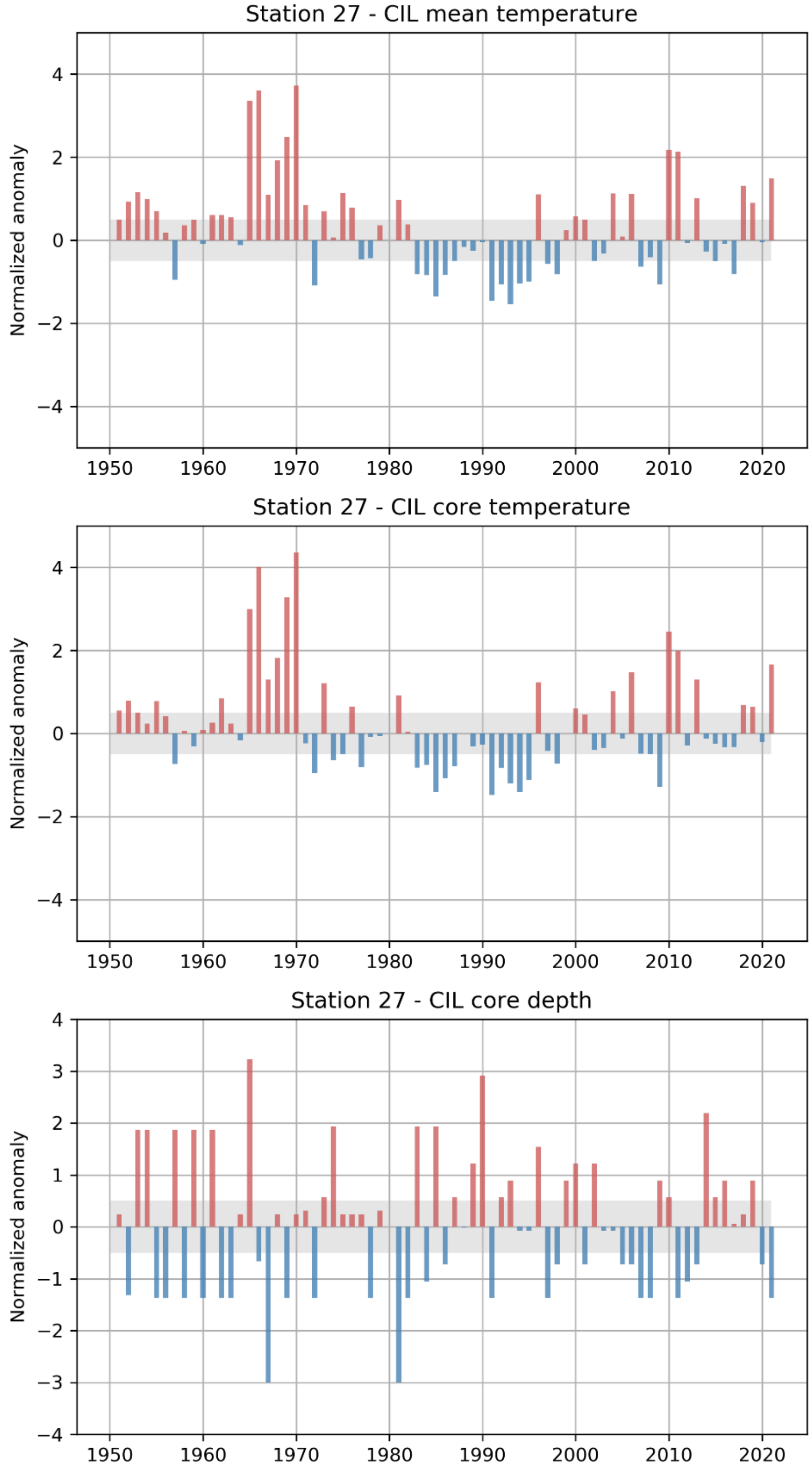

Figure 21: Normalized anomalies of summer (May-July) cold intermediate layer (CIL) statistics at Station 27 since 1951. Only years wehre at least 8 months of the years are sampled are presented. The top panel shows the CIL mean temperature, the middle the CIL core temperature (minimum temperature of the CIL) and the bottom panel the depth of the CIL core. Shaded gray areas represent the climatological (1991–2020) average ±0.5 SD range considered "normal". The CIL core temperature anomalies (middle panel) contribute to the NL climate index described in the summary (Figure 40).

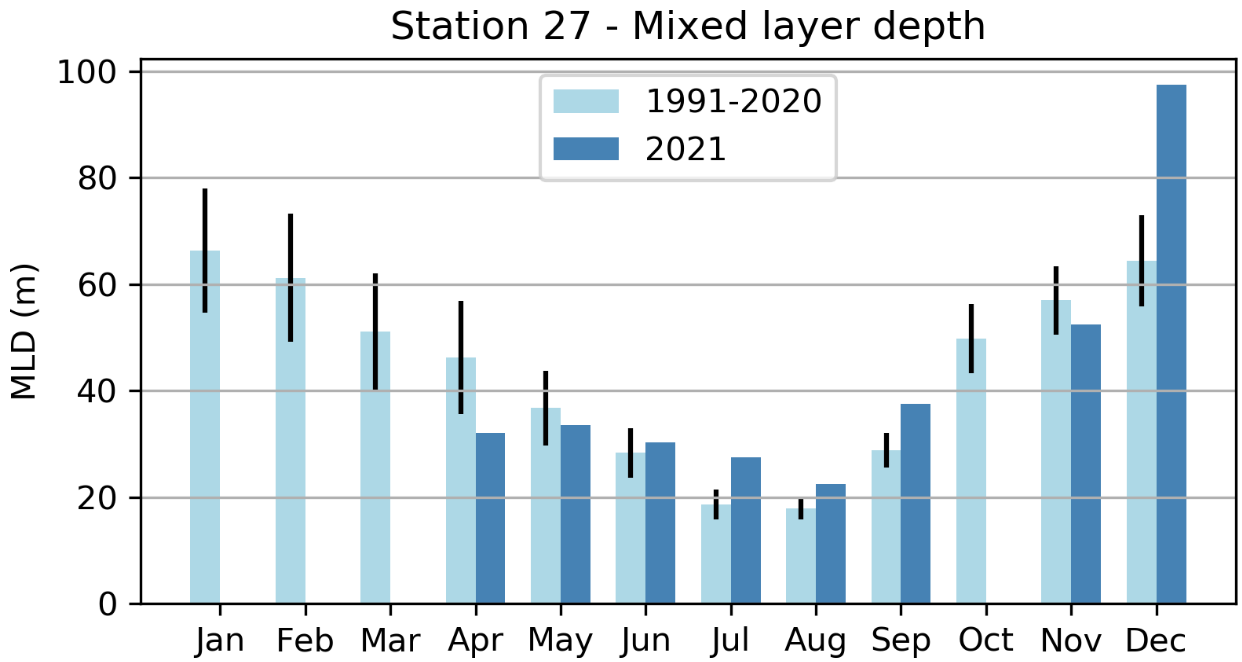

Figure 22: Bar plot of the monthly averaged mixed layer depth (MLD) at Station 27. The 1991–2020 climatology is shown in light blue while the update for 2021 is shown in dark blue. The black lines represent 0.5 SD above and below the climatology. No observations were made between January and March.

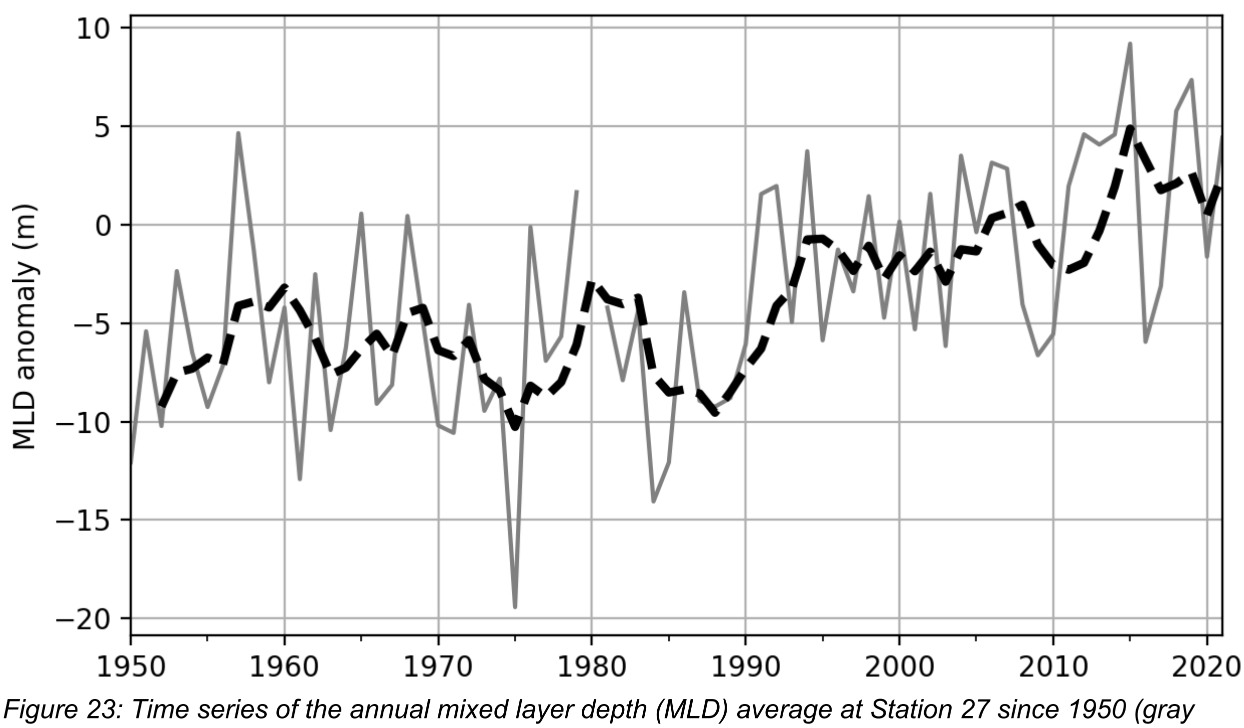

Figure 23: Time series of the annual mixed layer depth (MLD) average at Station 27 since 1950 (gray solid line) and its 5-year running mean (dashed-black line).

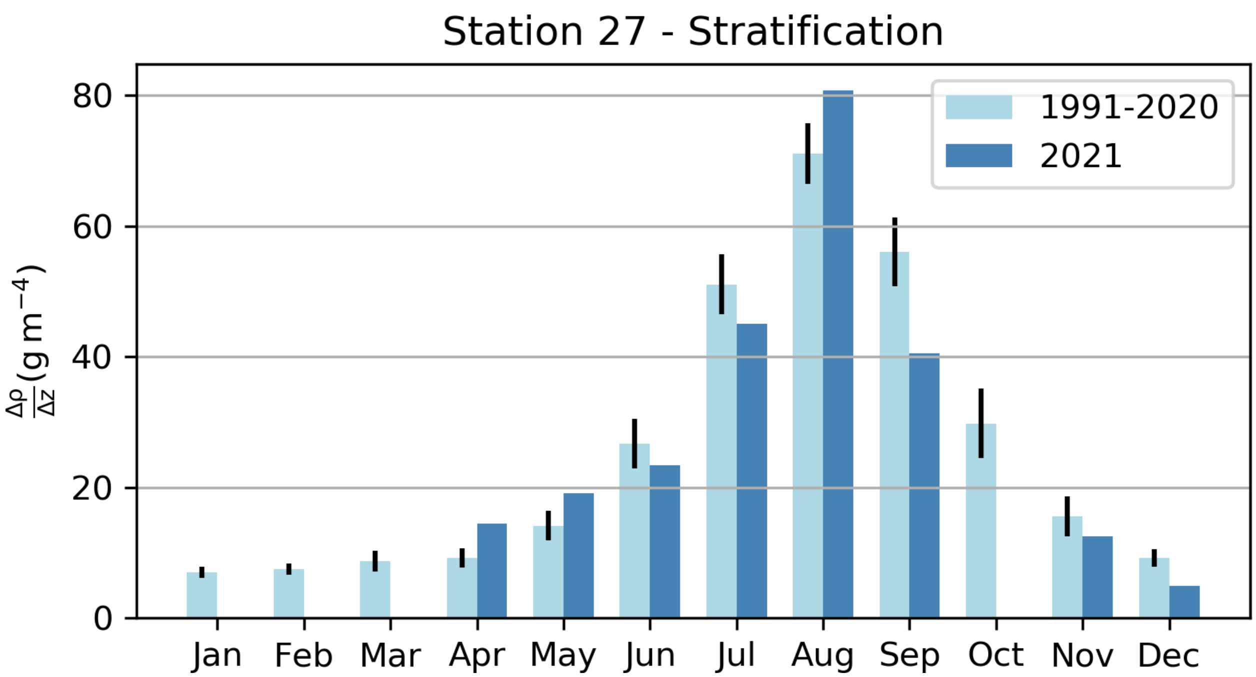

Figure 24: Bar plot of the monthly average stratification (defined as the density difference between 0 and 50 m) at Station 27. The 1991–2020 climatology is shown in light blue while the update for 2021 is shown in dark blue. The black lines represent 0.5 SD above and below the climatology. No observations were made between January and March.

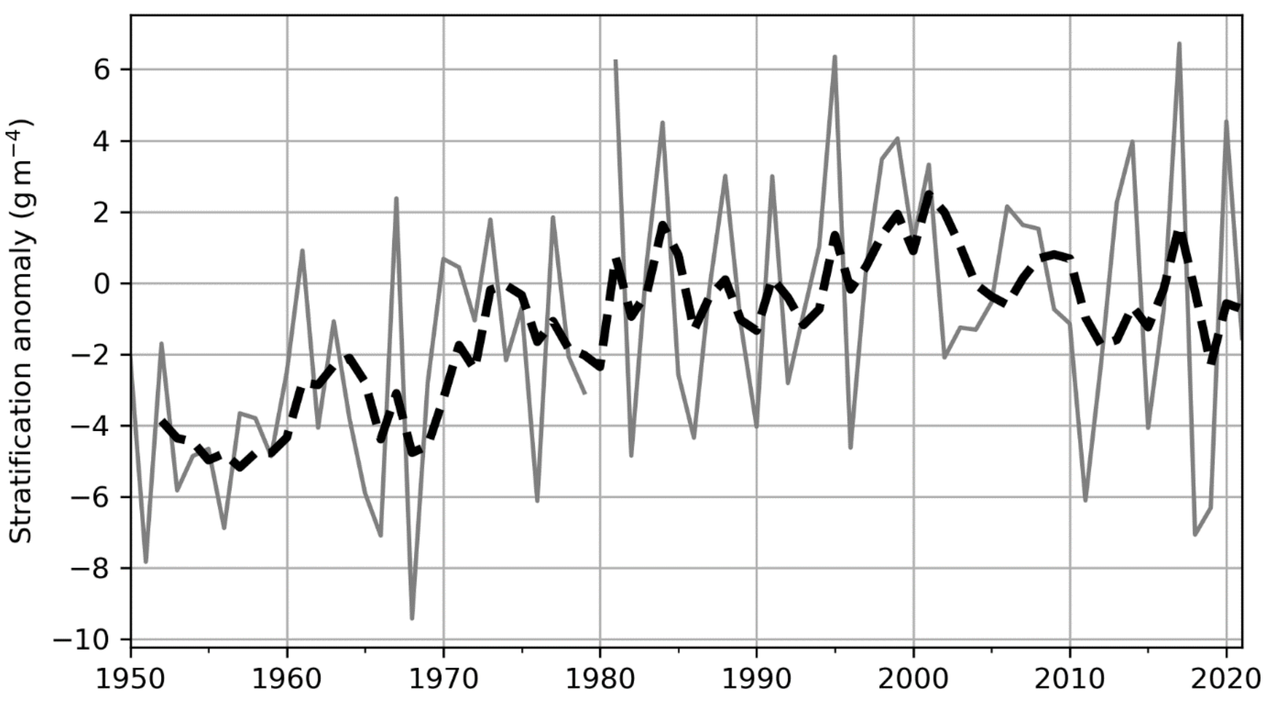

Figure 25: Time series of the annual average stratification at Station 27 since 1950 (gray solid line) and its 5-year running mean (dashed-black line).

STANDARD HYDROGRAPHIC SECTIONS

In the early 1950s, several countries under the auspices of the International Commission for the Northwest Atlantic Fisheries (ICNAF) carried out systematic monitoring along hydrographic sections in NL waters. In 1976, ICNAF normalized a suite of oceanographic monitoring stations along sections in the Northwest Atlantic Ocean from Cape Cod (USA) to Egedesminde (West Greenland) (ICNAF 1978). In 1998 under the AZMP, the Seal Island (SI), Bonavista Bay (BB), Flemish Cap (47°N) (FC) and Southeast Grand Bank (SEGB) historical stations were selected as core monitoring sections. The White Bay section (WB) continued to be sampled during the summer as a long time series ICNAF/NAFO section (see Figure 1).

Two ICNAF sections on the mid-Labrador Shelf, the Beachy Island (BI) and the Makkovik Bank (MB) sections, were selected to be sampled during the summer if survey time permitted. Starting in the spring of 2009, a section crossing south-west over St. Pierre Bank (SWSPB) and one crossing south-east over St. Pierre Bank (SESPB) were added to the AZMP surveys.

In 2021, both the spring and fall survey were canceled. In 2020, the spring survey was also canceled due to the COVID-19 pandemic. During the summer 2021 survey (June 29-July 19), section FC, BB, WB, SI and MB were sampled. In this manuscript we present the summer cross sections of temperature and salinity and their anomalies along the SI, BB and FC sections to represent the vertical temperature and salinity structure across the NL Shelf during 2021.

Temperature and Salinity Variability

The water mass characteristics observed along the standard sections crossing the NL Shelf are typical of Arctic-origin waters with a subsurface temperature range of -1.5°C to 2°C and salinities from 31.5 to 33.5. Labrador Slope water flows southward along the shelf edge and into the Flemish Pass and Flemish Cap regions. With temperatures in the range of 3°C to 4°C and salinities in the range of 34 to 34.75, this water mass is generally warmer and saltier than the shelf waters. Surface temperatures normally warm to between 10°C and 12°C during late summer, while bottom temperatures remain <0°C over much of the Grand Banks, increasing to between 1°C and 3.5°C near the shelf edge below 200 m and in the deep troughs between the banks. In the deeper (>1,000 m) waters of the Flemish Pass and across the Flemish Cap, bottom temperatures generally range from 3°C to 4°C. In general, the near-surface water mass characteristics along the standard sections undergo seasonal modification from annual cycles of air-sea heat flux, wind-forced mixing, and the formation and melting of sea ice. These mechanisms cause intense vertical and horizontal temperature and salinity gradients, particularly along the frontal boundaries separating the shelf and slope water masses. The seasonal changes in the temperature and salinity fields along the Bonavista section are presented in Colbourne et al. (2015).

The 2021 summer temperature and salinity structures along the SI, BB and FC; (along 47°N) hydrographic sections are presented in Figure 26 to Figure 28. The dominant thermal feature along these sections is associated with the cold and relatively fresh CIL overlying the shelf. This water mass is separated from the warmer and denser water of the continental slope region by strong temperature and salinity fronts. The cross sectional area (or volume) of the CIL is bounded by the 0°C isotherm and highlighted as a thick black contour in the temperature panels. The CIL parameters are generally regarded as robust indicators of ocean climate conditions on the eastern Canadian Continental Shelf. While the CIL area undergoes significant seasonal variability, the changes are highly coherent from the Labrador Shelf to the Grand Banks. The CIL remains present throughout most of the summer until it gradually decays during the fall as increasing winds and storm episodes deepen the surface mixed layer.

During 2021, temperatures were above normal for all sections and most depth ranges (Figure 26 to Figure 28, bottom left). The conditions were also getting warmer from north to south, reaching more than 3.5°C above normal in most of the FC section. Warmer than normal temperatures were also found near the bottom at all sections. The latter information is important to note because, as presented in the next section, the reduced coverage of the multi-species survey in 2021 prevented the calculation of spring and fall bottom temperatures in large areas of the NL shelf, including on the Grand Banks of Newfoundland, an area crossed by section FC. The observations made during AZMP missions show widespread warmer than normal temperatures. This is important and will be discussed further.

The corresponding salinity cross sections show a relatively fresh (<33) upper water layer over the shelf with sources from Arctic outflow on the Labrador Shelf, in contrast to the saltier Labrador Slope water further offshore with values >34 (Figure 26 to Figure 28, right panels). In 2021, salinities corresponding to the CIL were slightly lower than normal for all sections, while the slope waters were above normal. The latter is likely due to an unusual extension of the saltier Labrador Current onto the slope in 2021 compared to the climatology. This is especially evident for sections SI and FC (see the difference in the salinity field between the top two right panels of all three figures). The fresher waters on the shelf (see also the large fresh anomaly at Station 27; Figure 19, bottom), may be related to the warm air temperature anomalies observed in Labrador and the Arctic in 2021.

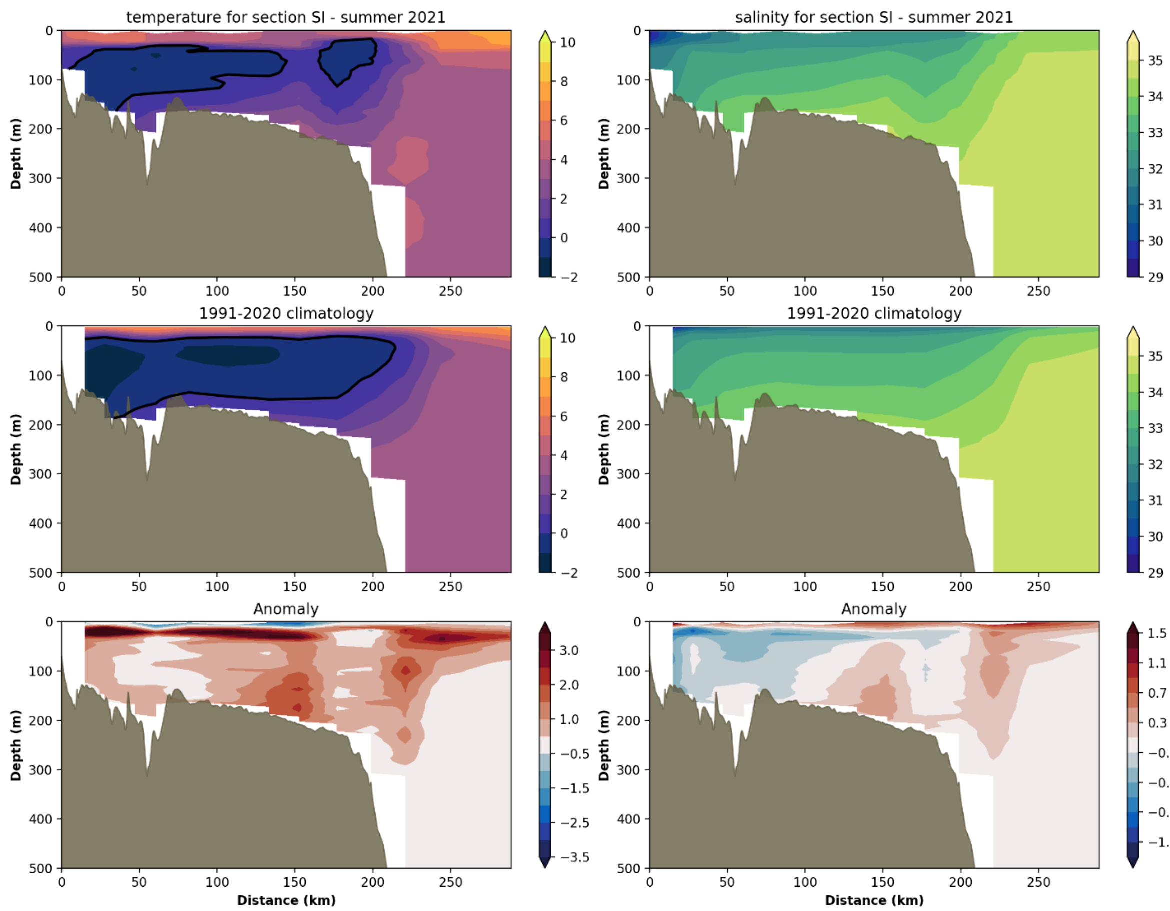

Figure 26: Contours of temperature (°C), left column, and salinity, right column, during summer 2021 (top row), with climatological averages (middle row) for the Seal Island (SI) hydrographic section (see map Figure 1 for location). Their respective anomalies for 2021 are plotted in the bottom panels.

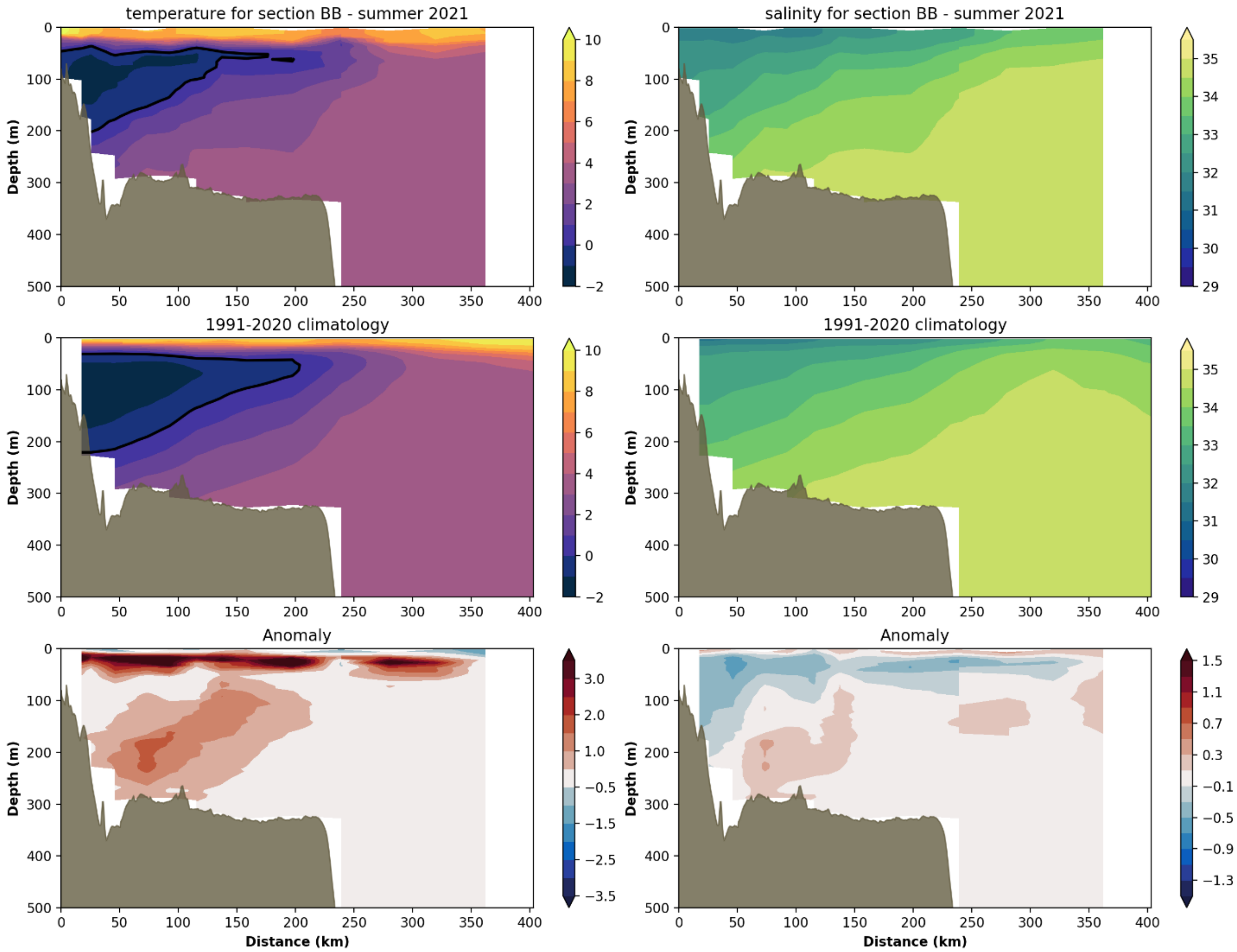

Figure 27: Same as in Figure 26, but for the Bonavista (BB) hydrographic section (see map Figure 1 for location).

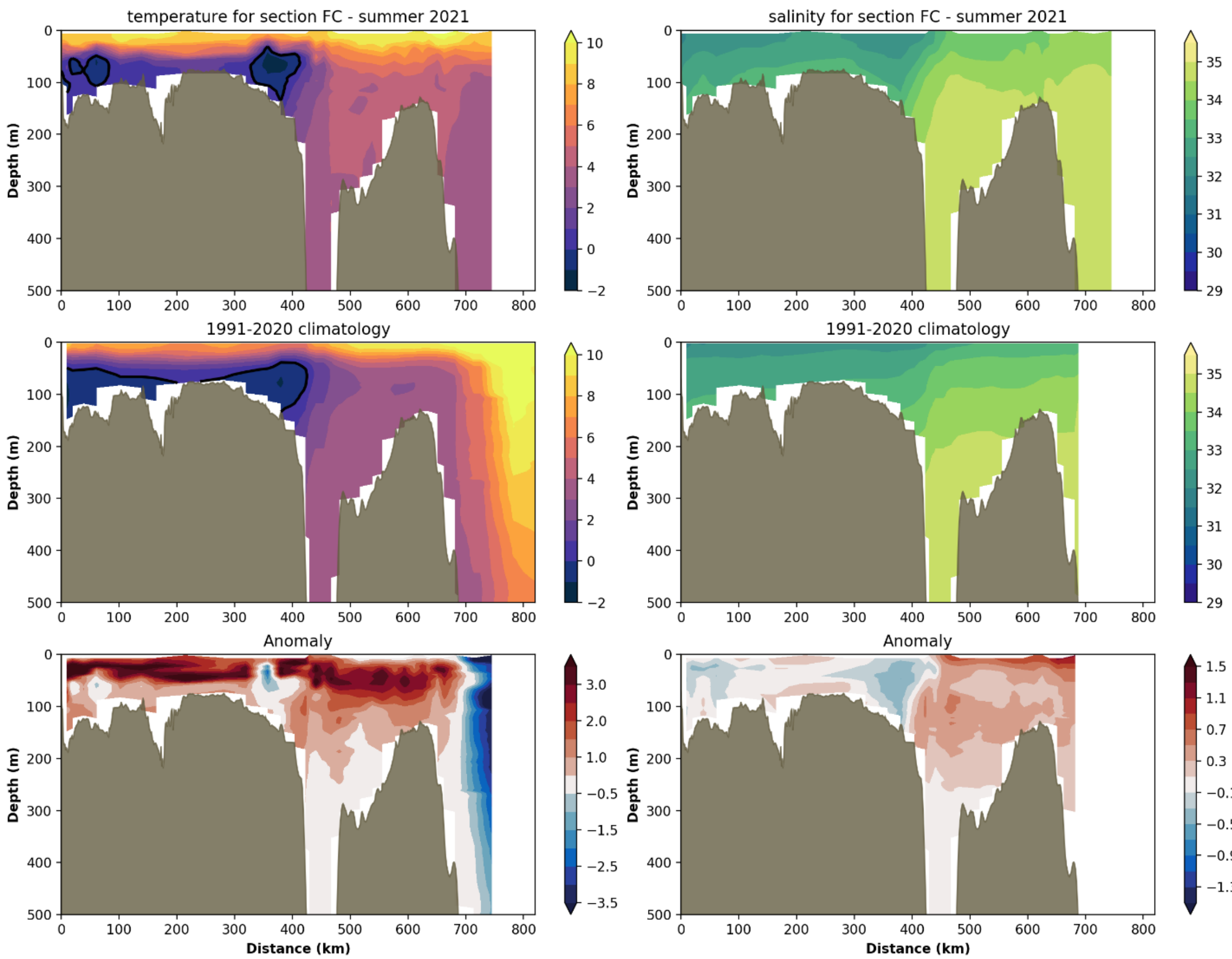

Figure 28: Same as in Figure 26, but for the Flemish Cap (FC) hydrographic section (see map Figure 1 for location).

Cold Intermediate Layer Variability

Statistics of summer CIL anomalies (CIL area, CIL core temperature and CIL core depth) for the three sections discussed above (SI, BB and FC) are presented in a scorecard in Figure 29. The climatological average cross sectional areas of the summer CIL along these sections are 19.9±4.1 km^2, 22.9±7.6 km^2 and 16.5±6.4 km^2, respectively. The averaged anomalies of the CIL cross-sectional area for these three sections are summarized in Figure 30 as a time series going back to 1950. In general, the summer CIL has been predominantly warmer and smaller than average since the mid-1990s, with a cooling trend emerging since about 2012 or 2014 to 2017. However, the most striking aspect of this long time series is the warm conditions that prevailed in the 1960s (that stands as a unique feature for this nearly 70-year time series, although measurements during this period were largely made from reversing thermometers that might have missed the CIL core), followed by a cold period that lasted from the mid-1980s to the mid-1990s. In 2021, the CIL conditions were much warmer than normal, including and north-south anomaly gradient, with warmest CIL condition on the northernmost section SI. On average over these three sections, 2021 is the year with the smallest CIL area since 1966 at -1.7 SD (Figure 30).

	80	81	82	83	84	85	86	87	88	89	90	91	92	93	94	95	96	97	98	99	00	01	02	03	04	05	06	07	08	09	10	11	12	13	14	15	16	17	18	19	20	21	$\bar{x}$	sd
-- Seal Island section --																																												
CIL area (km^2)	0.0		0.2	-0.3	2.0	0.7	-0.4	-0.1	-0.7		1.2	1.4	-0.1	1.7	0.0	-0.3	0.2	-0.7	0.5	-1.6	-0.1	0.5	0.0	0.9	-0.9	0.0	-0.5	0.1	0.2	0.6	-0.6	-1.2	0.6	-0.5	0.4	2.0	-0.1	1.9	-2.1	-0.4	-1.9	-2.1	19.9	4.1
CIL core (°C)	0.9		1.2	-0.4	-0.8	-0.1	2.2	1.7	1.3		-0.5	-0.5	0.0	-0.6	-0.5	-0.5	0.7	-0.5	-0.5	-0.5	-0.5	2.6	-0.5	1.8	-0.5	-0.5	-0.5	-0.5	-0.5	-0.5	2.6	-0.5	-0.5	2.6	-0.1	-0.5	-0.5	-0.5	-0.5	0.5	-0.5	3.7	-1.7	0.1
core depth (m)	1.1		1.3	0.0	1.3	-1.4	1.1	1.3	-0.3		0.4	0.4	0.0	-1.2	0.4	0.4	-1.8	0.4	0.4	0.4	0.4	-2.3	0.4	0.6	0.4	0.4	1.3	0.4	0.4	0.4	-2.7	0.4	1.1	-0.7	-1.2	1.1	0.4	0.4	0.4	-1.6	0.4	-1.6	87.4	22.5
-- Bonavista section --																																												
CIL area (km^2)	-0.4	-0.2	1.5	1.7	3.2	2.0	-0.4	-0.7	0.9	0.7	1.8	2.4	1.2	1.4	1.0	-0.2	0.2	-0.4	0.3	-0.4	0.7	-0.4	-0.4	0.1	-1.4	-0.8	-1.2	-0.3	-0.9	0.5	-0.3	-2.1	-0.2	-0.6	1.8	1.0	0.8	0.5	-0.4	-0.9	-1.2	-1.4	22.9	7.6
CIL core (°C)	1.2	0.6	-0.3	-1.7	-1.2	-1.0	0.3	-0.7	0.5	-1.0	-0.9	-1.3	-1.1	-1.1	-1.2	-0.6	0.8	-0.6	-0.6	0.0	-0.2	0.5	-0.1	-0.3	1.8	0.9	2.0	0.0	-0.3	-0.7	0.8	2.5	-0.8	0.4	-0.9	-1.0	-0.6	-0.8	0.8	0.4	1.2	1.5	-1.6	0.1
core depth (m)	0.5	-0.8	0.4	1.4	-1.5	-1.3	-0.1	1.4	-0.1	0.2	1.9	-1.3	0.4	1.1	0.4	-0.1	-0.3	-0.5	-1.3	0.7	0.9	-1.3	1.1	0.2	-0.5	-1.7	0.7	0.7	-0.1	-1.7	-1.7	0.2	1.1	-0.8	0.7	2.1	0.4	-0.5	-0.3	1.4	-0.1	-0.1	92.7	20.8
-- Flemish Cap section --																																												
CIL area (km^2)	-1.6	-0.3	-1.5	2.0	2.3	0.8	0.2	-1.2	-0.8	1.0	0.8	2.0	-0.5	1.7	0.0	-0.5	0.0	0.4	0.8	0.5	-1.1	-0.6	0.2	-0.5	-0.4	0.2	-1.5	-0.1	-1.1	0.4	-1.9	-0.9	0.8	-0.7	-0.2	-0.2	2.6	-0.9	0.1	1.3	0.2	-1.5	16.5	6.4
CIL core (°C)	0.0	1.1	-0.3	-0.9	-0.9	-0.9	-0.7	-0.9	0.4	-1.2	-0.5	-1.1	-0.8	-1.1	-0.6	-1.4	1.2	0.1	-0.5	0.4	0.2	1.4	-0.8	-0.2	0.7	0.3	0.6	-0.4	-0.2	-0.9	2.4	1.9	-1.0	2.3	-0.8	-1.0	-0.2	0.2	-0.4	0.3	-0.7	-0.2	-1.5	0.2
core depth (m)	1.4	2.9	1.4	-0.4	-1.0	0.1	0.6	0.9	3.0	-0.2	0.3	-1.0	-1.7	-0.4	0.6	1.4	-1.0	-1.0	0.3	1.1	-0.2	1.1	-0.4	0.9	0.6	-0.4	0.6	-0.2	-1.0	2.2	-1.0	-0.7	-0.2	1.1	-1.0	0.9	0.3	-1.7	1.6	-0.4	-0.4	-0.7	75.0	19.3

Figure 29: Scorecards of the cold intermediate layer (CIL) summer statistics along the Seal Island, Bonavista and Flemish Cap hydrographic sections. The CIL area is defined as all water below 0°C (see black contours in Figure 26 to Figure 28), and the CIL core temperature and depth are the minimum temperature of the CIL and the depth at which it is encountered, respectively. Color codes for the area and depth have been reversed (positive is blue and negative is red) because they represent cold conditions. Grayed cells indicate an absence of data.

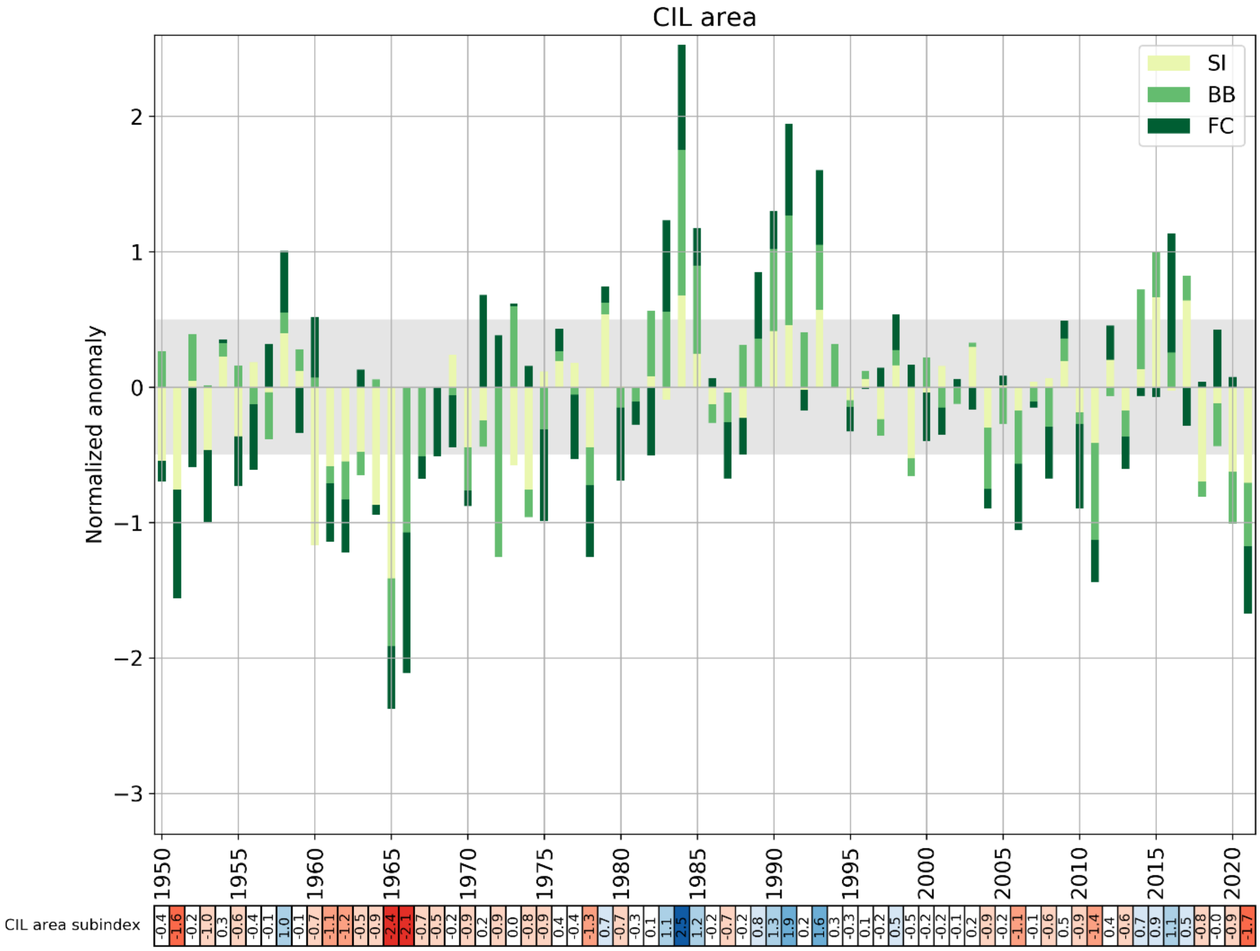

Figure 30: Normalized anomalies of the mean CIL area for hydrographic sections Seal Island (SI), Bonavista Bay (BB) and Flemish Cap (FC). This time series corresponds to the average of the three sections, in which the contribution of each section is represented (values for each separate section since 1980 can be found in Figure 29). The shaded area corresponds to the 1991–2020 average ±0.5 SD, a range considered "normal". The numerical values of this time series are reported in a color-coded scorecard at the bottom of the figure. Here negative anomalies (generally corresponding to warmer conditions) are colored red and positive anomalies blue. This time series is one component of the NL climate index (Figure 40).

BOTTOM OBSERVATIONS IN NAFO SUB-AREAS

Canada has been conducting stratified random bottom trawl surveys in NAFO Sub-areas 2 and 3 on the NL Shelf since 1971. Areas within each division, with a selected depth range, were divided into strata, and the number of fishing stations in an individual stratum was based on an area-weighted proportional allocation (Doubleday 1981). Temperature profiles (and since 1990, salinity profiles) are available for most fishing sets in each stratum. These surveys provide large spatial-scale oceanographic data sets for the Newfoundland and Labrador Shelf. NAFO Subdivision 3Ps on the Newfoundland south coast and Divisions 3LNO on the Grand Banks are surveyed in the spring, and Divisions 2HJ off Labrador in the north, 3KL off eastern Newfoundland, and 3NO on the southern Grand Bank are surveyed in the fall. The hydrographic data collected on these surveys are routinely used to assess the spatial and temporal variability in the thermal habitat of several fish and invertebrate species. A number of products based on the data are used to characterize the oceanographic bottom habitat. Among these are contour maps of the bottom temperatures and their anomalies, the area of the bottom covered by water in various temperature ranges, etc. In addition, species-specific 'thermal habitat' indices are often used in marine resource assessments for snow crab and northern shrimp.

The current method to derive the bottom temperature was introduced by Cyr et al. (2019) and is similar to the approach presented in reports of the annual physical oceanographic conditions for the Gulf of St. Lawrence (e.g., Galbraith et al. in prep[1]). First, all available annual profiles of temperature and salinity (from AZMP hydrographic campaigns, multi-species resources assessments, surveys from other DFO regions, international oceanographic campaigns, Argo program, etc.) are vertically averaged in 5 m bins and linearly interpolated to fill missing bins. Then, for each season (April-June for spring and September-December for fall), all data are averaged on a regular 0.1° x 0.1° (latitudinal x longitudinal) grid to obtain one seasonal profile per grid cell. Since this grid has missing data in many cells, each depth level is horizontally linearly interpolated. For each grid point, the bottom observation is considered as the data at the closest depth to the GEBCO_2014 Grid bathymetry (version 20141103), to a maximum 50 m difference. Lastly, bottom observations deeper than 1,000 m are clipped as they are down the continental slope in a depth range with much lower data coverage. This method is applied for all years between 1980 and 2021 from which the 1991–2020 climatology is derived. Anomalies for 2021 are calculated as the difference between annual observations and the climatology.

Spring Conditions

Maps of spring climatological temperature and salinity, together with 2021 observations and anomalies for NAFO divisions 3LNOPs, are presented in Figure 31 and Figure 32, respectively (with the center panel for station occupation coverage). Due to the COVID-19 pandemic, the area was not surveyed during the spring of 2020, while in 2021 only the division 3Ps was properly sampled. Temperatures were generally above 0°C over the shallower St. Pierre Bank (eastern 3Ps) and above 6°C in the deep Laurentian Channel, leading to widespread warm anomalies over this division, especially in the shallower part where temperatures 1.5 to 2.5°C above the climatological mean (Figure 31, right panel).

Spring bottom salinities in 3LNO generally range from 32 to 33 over the central Grand Bank, and from 33 to 35 closer to the shelf edge (Figure 32, left panel). In 3Ps, salinities were between 32 and 33 over shallower areas and above 34.5 in the Laurentian Channel. In 2021, salinity conditions were close to normal in 3Ps (Figure 32, right panel).

Climate indices based on normalized spring bottom temperature anomalies (mean temperature and temperature in areas shallower than 200 m), as well as the area of the sea floor covered by water above 2°C and below 0°C between 1980 and 2021 are shown in a color-coded scorecard in Figure 33. Overall, the colors visually highlight two contrasting periods of this time series: the cold period of the late 1980s / early 1990s (mostly blue cells) and the warm period of the early 2010s (mostly red cells). This warm period lasted between 2010 and 2013 (2011 being the warmest at 2.1 SD above normal in 3LNO) before returning towards to normal values. Between 2015 and 2017 the bottom area that was covered by <0°C water was normal at -0.2 to 0.4 SD.

Division 3Ps bottom temperatures exhibit some similarities to those from 3LNO, with two periods of warm years, 1999–2000 and 2005–06, separated by a colder period (2003 is the coldest year on record since 1991 at -2.1 SD). With the exception of 2014 and 2017 (normal), all years between 2010 and 2021 were warmer than normal. As mentioned above, very little information is available for 2020 and 2021. In 3Ps, the only division with available data, 2021 was the warmest year on record since 1980 at +2.0 SD. 2021 was also the year with the smallest area of the seafloor covered by water <0°C at -1.5 SD (tied with 2011).

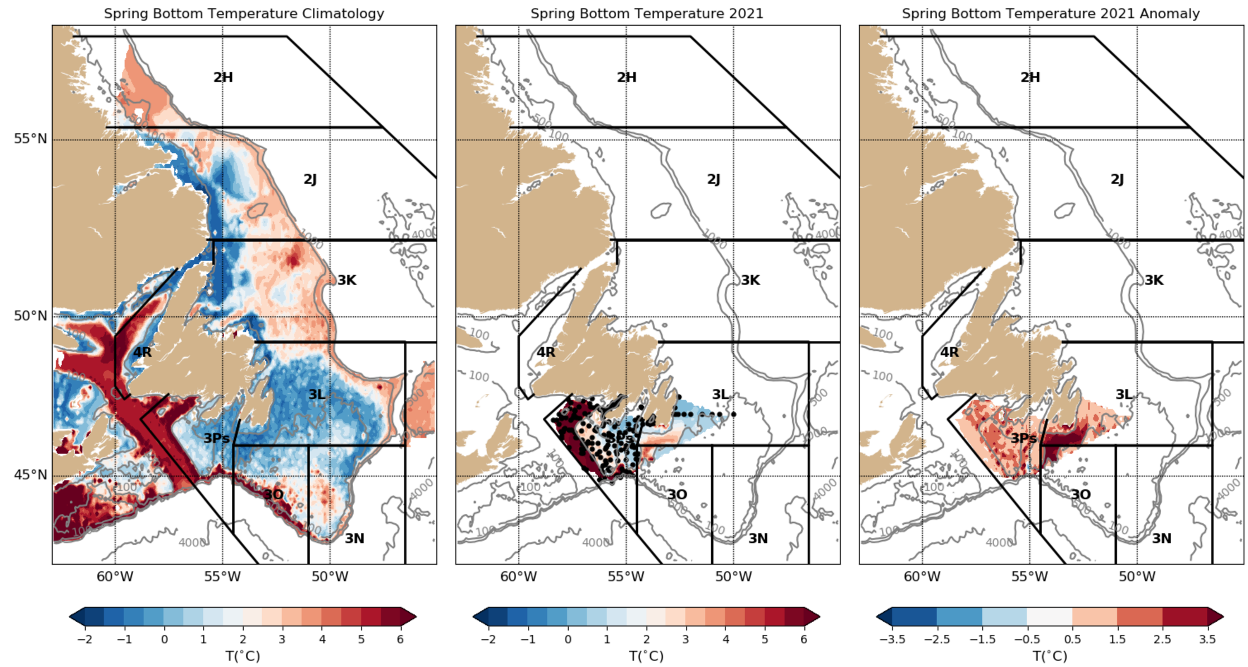

Figure 31: Maps of the climatological (1991–2020) mean spring bottom temperature (left), and spring 2021 bottom temperature (center) and anomalies (right) for NAFO Divisions 3LNOPs only. The location of observations used to derive the temperature field is shown as black dots in the center panel.

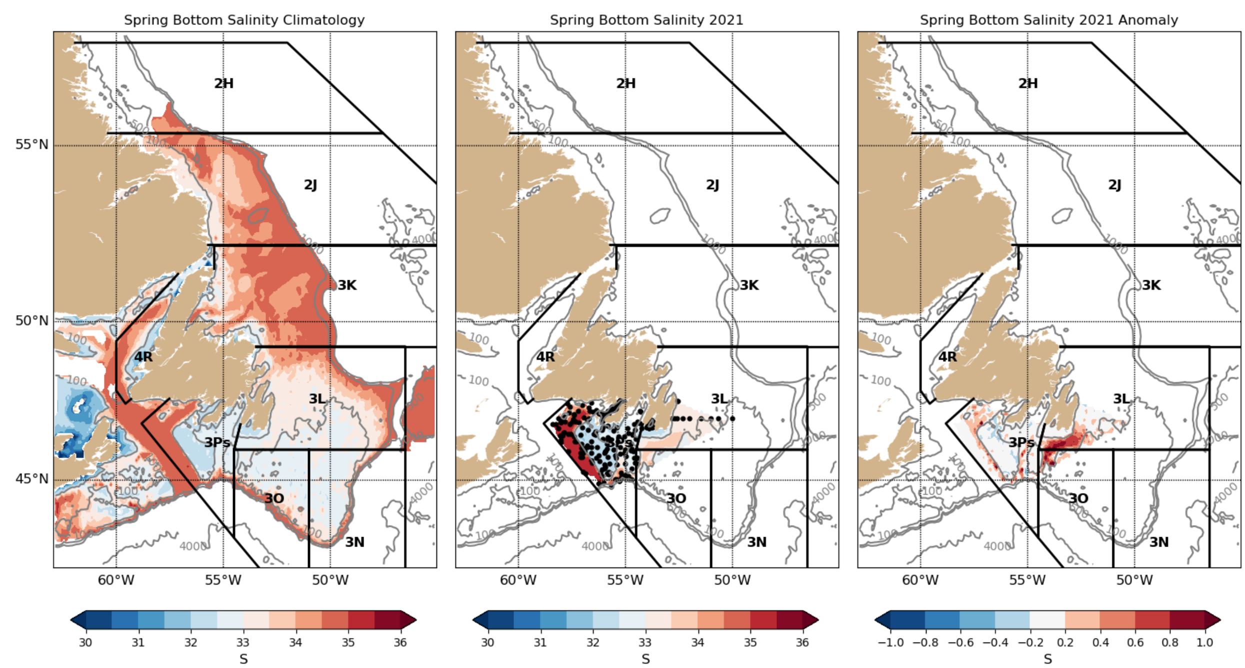

Figure 32: Maps of the climatological (1991–2020) mean spring bottom salinity (left), and spring 2021 bottom salinity (center) and anomalies (right) for NAFO Divisions 2J3KLNO only. The location of observations used to derive the salinity field is shown as black dots in the center panel.

	80	81	82	83	84	85	86	87	88	89	90	91	92	93	94	95	96	97	98	99	00	01	02	03	04	05	06	07	08	09	10	11	12	13	14	15	16	17	18	19	20	21	$\bar{x}$	sd
-- NAFO division 3LNO --																																												
T_{bot}	-0.1	1.4	-0.8	0.4	-0.9	-1.5	-1.3	-0.5	0.0	-1.4	-2.1	-2.1	-1.7	-1.3	-1.6	-0.8	-0.1	-0.9	0.6	1.2	0.6	0.0	-0.2	-1.1	1.3	0.6	0.5	0.2	0.1	0.2	0.9	2.1	1.4	1.1	-0.5	-0.1	-0.6	-0.1	0.2	0.2			1.1	0.5
$T_{bot_{<200m}}$	-0.3	1.6	-0.6	0.7	-0.9	-1.5	-1.3	-0.4	0.0	-1.2	-2.0	-2.0	-1.7	-1.2	-1.6	-0.9	0.0	-1.0	0.6	1.4	0.7	0.0	-0.2	-1.3	1.3	0.5	0.4	0.1	0.0	0.2	0.8	2.1	1.4	1.1	-0.6	-0.1	-0.3	-0.2	0.2	0.3			0.7	0.6
$Area_{>2°C}$	-0.2	1.3	-1.5	0.6	-0.7	-1.6	-1.2	-0.4	0.0	-1.4	-2.1	-1.8	-1.8	-1.1	-1.4	-0.4	-0.1	-0.8	0.4	1.2	0.4	-0.6	-0.3	-1.0	1.8	0.6	0.3	0.3	0.5	0.7	0.4	2.4	1.5	0.4	-0.4	0.3	-1.0	0.0	-0.3	-0.1			69.3	20.8
$Area_{<0°C}$	-0.3	-1.1	0.2	0.3	1.0	1.4	1.2	0.9	0.5	1.1	1.6	1.9	1.4	1.4	1.3	0.8	0.0	0.9	-0.6	-1.1	-0.1	0.0	0.2	1.0	-1.7	-0.7	-1.4	0.2	0.2	0.5	-1.6	-1.9	-0.8	-1.0	0.8	0.4	0.3	0.2	-0.2	-0.2			90.0	43.6
-- NAFO division 3Ps --																																												
T_{bot}			-0.5	0.1	0.2									-1.3	-1.3	-0.8	-0.2	-1.2	-0.2	0.8	1.1	-1.3	-0.5	-2.1	-0.4	0.6		-1.4	-0.3	0.2	0.5	1.4	1.2	0.7	0.3	0.5	1.6	0.3	1.1	0.7		2.0	2.4	0.5
$T_{bot_{<200m}}$			0.2	0.5	0.9									-1.8	-1.5	-0.9	-0.1	-1.3	0.1	1.1	1.3	-1.0	-0.6	-2.0	0.0	1.0		-0.9	0.2	0.5	0.4	1.5	0.9	0.8	0.2	0.4	1.2	-0.4	0.9	0.0		1.8	0.9	0.6
$Area_{>2°C}$			0.6	1.5	-1.0									-0.2	-0.5	0.5	-0.4	-0.7	0.6	2.4	2.0	-1.5	-0.7	-1.6	-1.0	0.1		-1.1	0.1	-0.1	0.1	1.8	0.2	0.5	-0.5	-0.2	-0.1	-0.3	1.4	-0.6		1.9	26.5	3.0
$Area_{<0°C}$			-0.2	-0.4	-0.7									1.7	1.3	1.2	-0.3	1.5	0.1	-0.5	-0.9	0.8	0.4	2.2	-0.8	-1.2		0.7	0.2	-0.1	-0.7	-1.5	-1.2	-1.2	-0.2	-0.6	-0.9	0.4	-0.8	0.4		-1.5	14.2	9.8

Figure 33: Scorecards of normalized spring bottom temperature anomalies (mean temperature, mean temperature for area shallower than 200 m, and area of sea floor covered by water above 2°C and below 0°C, respectively) for 3LNO and 3Ps.

Fall Conditions

Maps of fall climatological temperature and salinity, together with 2021 observations and anomalies for NAFO Divisions 2HJ3KLNO, are presented in Figure 34 and Figure 35 respectively (see center panel for station occupation coverage). Similar to the spring, Divisions 3LNO (Grand Banks) were not sampled due to ship availability problems. For the divisions where the data are available, a widespread warm anomaly was observed (Figure 34, right panel).

Bottom salinities in divisions 2HJ and 3K generally display an inshore-offshore gradient between <33 close to the coast and 34 to 35 at the shelf edge (Figure 35, left panel). The Grand Banks bottom salinities range from <33 to 35, with the lowest values on the southeast shoal. In 2021 the bottom salinities were slightly above normal in most of 2HJ3K (Figure 35, right panel), suggesting that the fresh anomaly observed at Station 27 (Figure 19, bottom panel) was driven by the upper parts of water column.

Normalized bottom temperature anomalies (mean temperature and temperature in areas shallower than 200 m), as well as area of the sea floor covered by water above 2°C and below 1°C between 1980 and 2021 are shown in a color-coded scorecard in Figure 36. A clear cold period is visible from the early 1980s to the mid-1990s, with the coldest anomalies reached in NAFO Divisions 2J and 3K. This was followed by a warmer period peaking in 2010 and 2011, the warmest years on records for these divisions. After a slight return to normal-to-cold anomalies between 2012 and 2017, bottom temperatures have been generally above normal since. In 2021, they were respectively 0.8 SD, 0.8 SD and 0.7 SD for NAFO Divisions 2H, 2J and 3K, respectively.

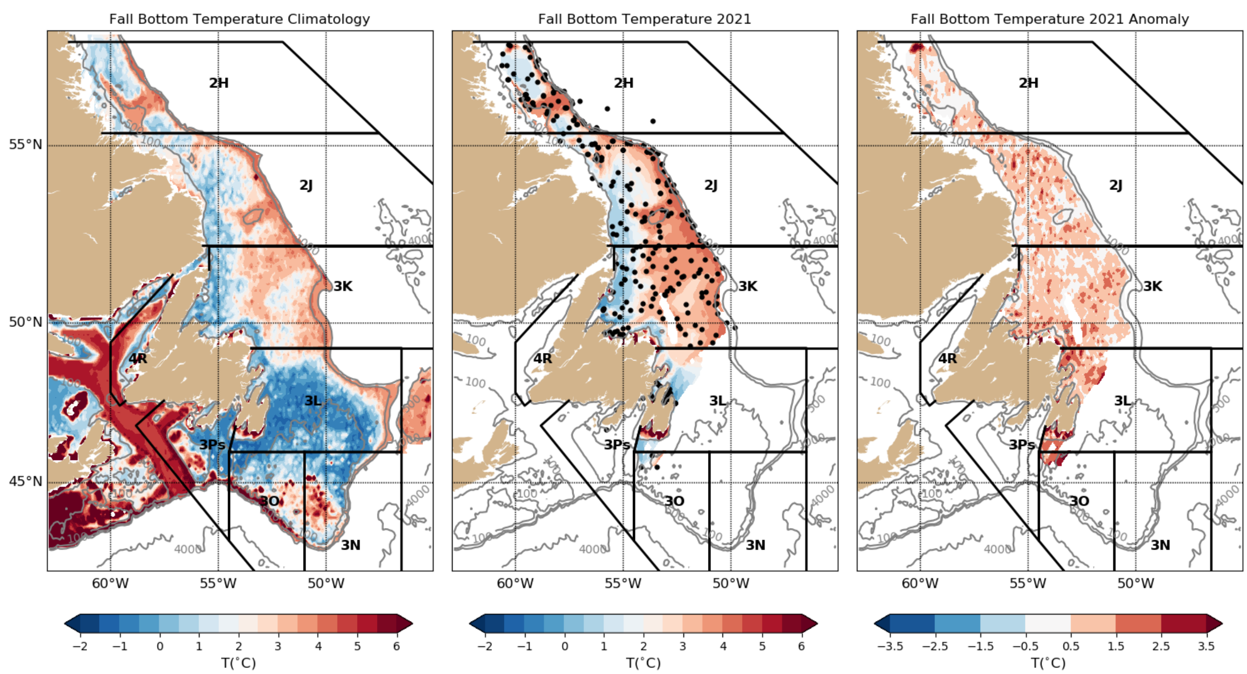

Figure 34: Maps of the climatological (1991–2020) mean fall bottom temperature (left), and fall 2021 bottom temperature (center) and anomalies (right) for NAFO Divisions 2HJ3KLNO only. The location of observations used to derive the temperature field is shown as black dots in the center panel.

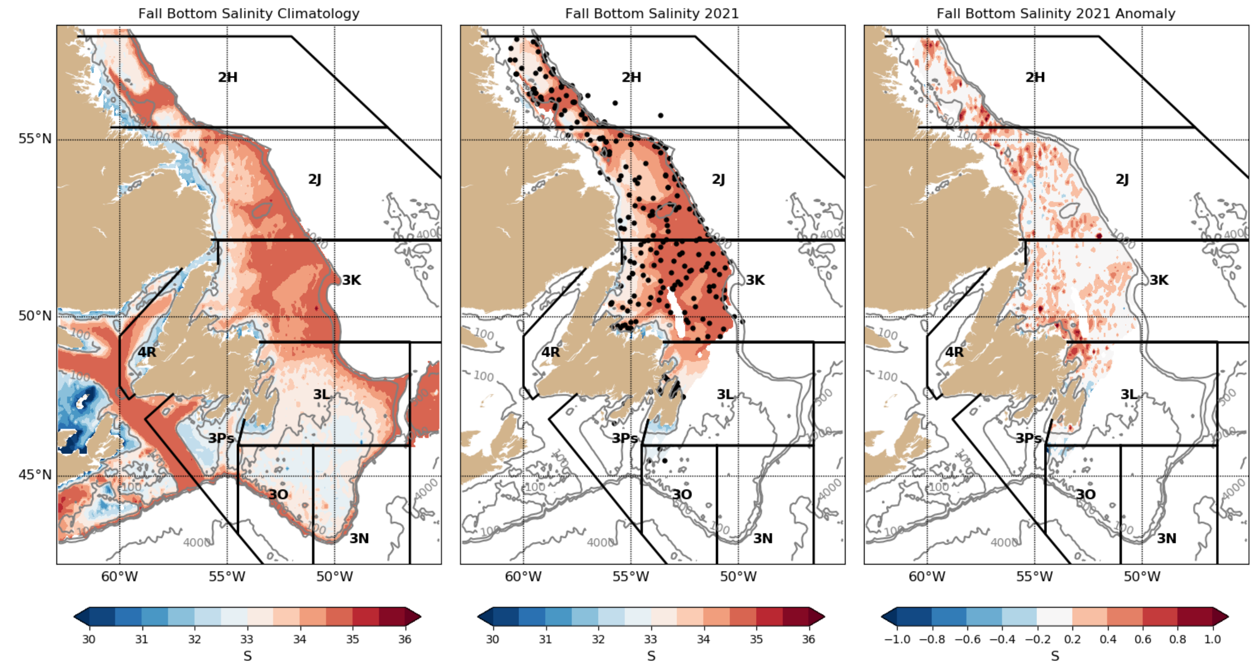

Figure 35: Maps of the climatological (1991–2020) mean fall bottom salinity (left), and fall 2021 bottom salinity (center) and anomalies (right) for NAFO Divisions 2HJ3KLNO only. The location of observations used to derive the salinity field is shown as black dots in the center panel.

	80	81	82	83	84	85	86	87	88	89	90	91	92	93	94	95	96	97	98	99	00	01	02	03	04	05	06	07	08	09	10	11	12	13	14	15	16	17	18	19	20	21	x̄	sd
-- NAFO division 2H --																																												
T_{bot}		-0.5		-3.2								-2.2						-0.2	-0.2	0.2		-0.5			1.2		-0.3		0.1		1.8	2.0	0.3	-0.4	-0.1	-0.6	-0.4	-1.6	0.2	0.2	0.3	0.8	2.3	0.4
$T_{bot<200m}$		0.4		-2.7								-2.0						0.6	0.2	0.4		-1.5			1.0		-0.6		-0.6		1.5	1.9	0.4	-0.8	-0.5	0.1	0.0	-1.4	0.3	0.4	0.7	0.8	1.1	0.5
$Area_{>2°C}$		-0.3		-1.4								-1.0						0.7	0.7	0.3		-1.2			1.5		0.0		-0.2		1.6	2.0	-0.2	-0.2	-0.5	-1.6	-0.4	-1.6	0.2	0.0	-0.2	0.1	20.9	4.1
$Area_{<1°C}$		-0.9		2.9								2.6						-0.9	0.6	-0.6		0.4			-0.7		0.9		0.9		-1.3	-1.4	-0.2	0.9	0.1	-0.1	-0.1	1.0	-0.5	-0.7	-1.0	-1.0	9.9	7.3
-- NAFO division 2J --																																												
T_{bot}	-0.8	-0.2	-1.7	-1.6	-2.9	-2.4	-0.2	-2.1	-0.4	-0.9	-1.9	-1.4	-2.3	-2.3	-1.6		0.3	0.0	0.0	0.3	-0.5	0.5	0.1	0.6	1.0	1.2	-0.4	1.2	-0.1	0.1	1.7	1.7	-0.1	0.0	-0.7	-0.7	0.2	-0.3	0.8	0.8	0.0	0.8	2.3	0.5
$T_{bot<200m}$	-0.4	0.0	-1.3	-1.8	-2.5	-1.8	0.0	-1.8	-0.3	-0.9	-1.5	-1.5	-2.1	-2.0	-1.3		0.5	-0.2	-0.2	0.4	-0.5	0.7	0.3	0.6	0.7	1.2	-0.7	1.2	-0.2	0.1	1.5	1.7	-0.3	-0.4	-1.0	-0.8	0.8	-0.3	0.6	1.2	0.0	0.6	1.0	0.7
$Area_{>2°C}$	-0.5	-0.3	-1.8	-1.1	-2.2	-2.0	-0.1	-1.7	-0.4	-1.0	-1.8	-1.2	-1.6	-1.9	-1.3		0.7	0.1	-0.2	-0.3	-0.5	0.6	-0.6	0.5	0.9	1.4	-0.3	1.5	-0.7	-0.3	1.9	2.2	-0.6	-0.3	-0.7	-0.5	0.2	-0.4	0.6	0.9	0.1	0.4	52.4	13.3
$Area_{<1°C}$	0.5	-0.1	1.8	1.7	2.2	2.0	-0.1	2.1	-0.1	1.0	1.8	1.6	1.9	2.0	1.4		-0.4	-0.1	0.3	-0.8	0.5	-0.7	-0.5	-0.7	-0.5	-1.3	0.7	-1.2	0.6	-0.1	-1.3	-1.3	0.5	0.4	1.0	0.8	-1.1	0.4	-0.6	-1.3	-0.2	-0.7	19.5	14.6
-- NAFO division 3K --																																												
T_{bot}	-0.3	-0.4	-0.6	-1.0	-1.7	-2.6	-0.5	-1.5	-0.8	-0.7	-2.2	-1.3	-2.2	-2.2	-1.7	-1.1	-0.4	0.3	0.2	0.6	0.2	-0.2	0.4	0.5	1.3	0.7	0.0	0.8	0.5	0.0	1.4	2.1	0.1	0.3	-0.5	-0.2	-0.5	-0.9	0.6	0.7	0.5	0.7	2.6	0.4
$T_{bot<200m}$	-0.2	-0.5	-2.2	-1.9	-2.1	-2.0	-0.2	-1.8	-1.1	-0.9	-1.8	-1.7	-1.8	-2.0	-1.6	0.0	0.4	-0.3	-0.6	0.3	-0.6	0.2	0.4	0.4	1.1	0.7	-0.3	0.9	-0.3	-0.2	1.8	1.6	-0.1	-0.5	-0.9	-0.3	0.9	-0.5	0.8	1.5	1.0	0.8	0.6	0.7
$Area_{>2°C}$	-0.3	-0.1	-0.3	-1.1	-1.4	-2.7	-0.2	-1.5	-0.8	-0.8	-2.1	-1.0	-2.1	-2.1	-1.8	-1.5	-0.4	0.6	0.4	0.6	0.4	-0.2	0.8	0.2	1.0	0.9	0.0	0.8	0.5	-0.5	1.6	1.4	0.0	0.5	-0.7	-0.1	-0.8	-0.9	0.8	0.8	0.9	-0.3	77.7	13.0
$Area_{<1°C}$	0.3	0.1	0.6	1.2	1.4	2.6	-0.4	0.8	0.2	0.3	2.8	1.4	2.0	2.5	1.8	0.2	-0.5	0.1	0.2	-0.3	0.4	0.0	-0.6	0.0	-1.2	-0.9	0.4	-1.0	0.2	0.3	-1.3	-1.4	0.3	-0.2	0.6	0.1	-0.7	0.8	-0.9	-1.3	-0.9	-0.6	13.3	9.0
-- NAFO division 3LNO --																																												
T_{bot}	0.3	-0.1	1.0	0.1	-0.5	-1.0	0.0	-0.7	-1.1	0.1	-1.0	-1.4	-1.3	-2.0	-1.4	-0.3	0.1	-0.1	0.7	1.7	-0.3	0.0	0.0	-0.3	0.8	0.2	0.5	-0.1	-0.5	0.5	1.3	2.4	0.4	0.6	-0.8	-0.1	0.2	-2.1	0.2	0.1	1.1		1.2	0.5
$T_{bot<200m}$	0.5	-0.1	1.2	0.2	-0.4	-0.9	0.2	-0.7	-1.0	0.2	-0.7	-1.3	-1.1	-2.0	-1.3	-0.2	0.2	-0.2	0.7	1.8	-0.5	0.1	-0.1	-0.4	0.7	0.2	0.6	-0.3	-0.8	0.6	1.4	2.4	0.3	0.6	-0.9	-0.3	0.3	-2.0	0.1	0.2	1.2		0.8	0.5
$Area_{>2°C}$	0.1	-0.3	0.5	0.5	0.1	-1.4	0.1	-0.6	-1.5	0.7	-1.1	-1.0	-1.3	-1.8	-1.3	-0.5	-0.1	-0.1	1.0	2.1	-0.1	-0.1	-0.2	-0.4	0.5	0.1	0.2	-0.1	-0.7	0.5	1.2	2.3	0.7	0.7	-1.0	0.0	0.3	-2.0	-0.1	0.1	1.3		73.5	22.3
$Area_{<0°C}$	-0.6	0.8	0.1	0.8	1.1	0.4	0.0	0.5	0.4	0.2	0.6	1.4	1.1	2.0	1.4	-0.2	0.1	0.3	-0.2	-1.2	0.7	0.1	-0.3	0.0	-1.6	-0.5	-0.9	0.1	0.5	-0.1	-1.1	-2.5	0.2	0.0	0.0	0.2	0.3	2.0	-0.4	-0.1	-1.3		91.6	33.2

Figure 36: Scorecards of normalized fall bottom temperature anomalies (mean temperature, mean temperature for area shallower than 200 m, and area of sea floor covered by water above 2°C and below 0°C, respectively) for 2H, 2J, 3K and 3LNO.

Summary of bottom temperatures

When standardized anomalies of spring and fall bottom temperatures (first row of all scorecards in Figure 33 and Figure 36) are combined in a bar plot, the low frequency patterns of the bottom temperature on the NL shelf become apparent (Figure 37). The coldest period encompasses the mid-1980s to the mid-1990s. Such cold anomalies are not observed later in the time series. For example, despite a winter NAO index leading to colder conditions between about 2012 and 2017 (see section on meteorological conditions), the bottom temperature during these years was just back to normal, following the rather warm period of the mid-1990s to the mid-2010s. While 2011 is the warmest year on record for the bottom temperature (+1.8 SD), 2021 ranked second at +1.4 SD.

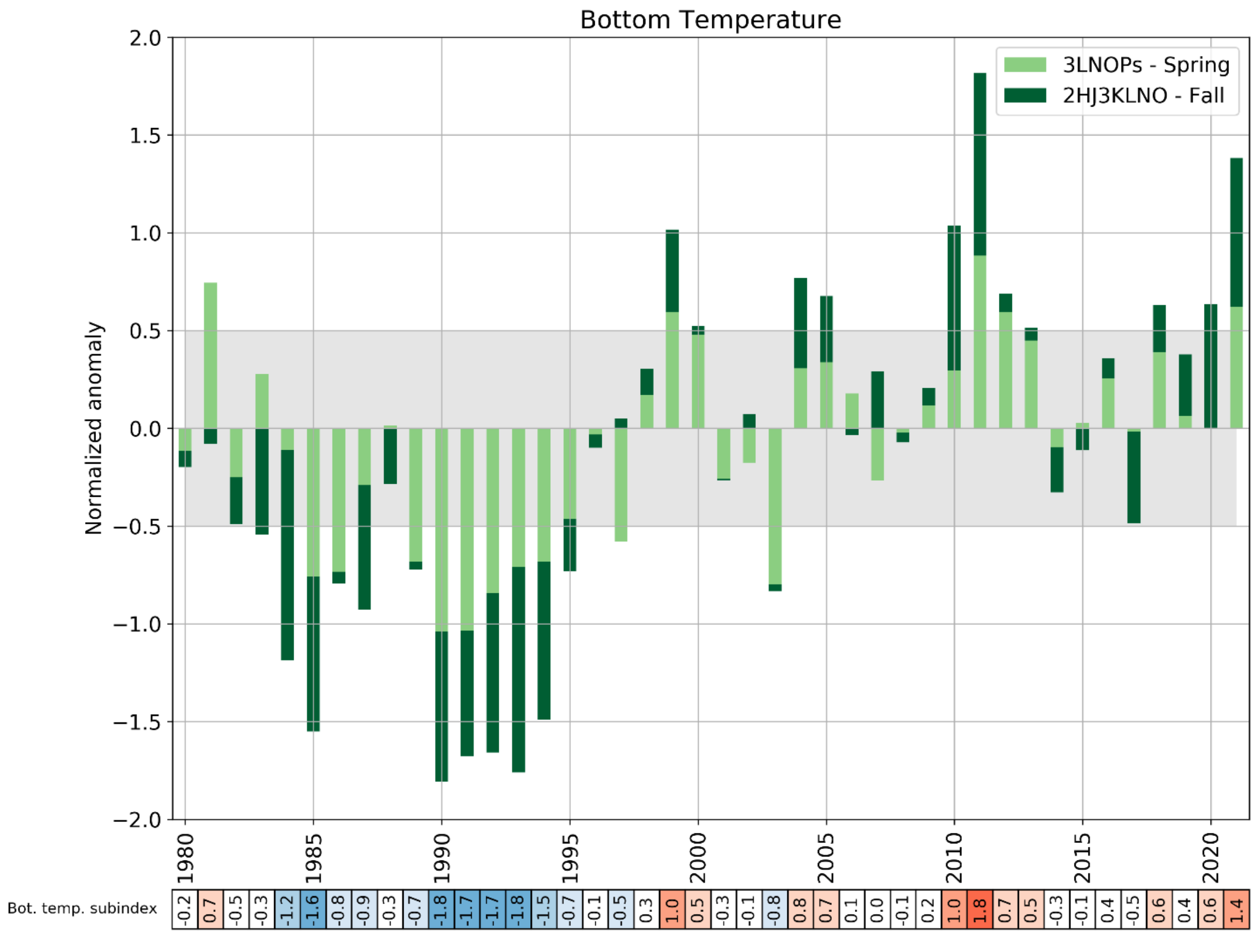

Figure 37: Normalized anomalies of bottom temperature in NAFO Divisions 3LNOPs (spring) and 2HJ3KLNO (fall). This time series corresponds to the average of the two seasons, in which each contribution is represented. The shaded area corresponds to the 1991–2020 average ±0.5 SD, a range considered "normal". The numerical values of this time series are reported in a color-coded scorecard at the bottom of the figure. This time series is one component of the NL climate index (Figure 40).

LABRADOR CURRENT TRANSPORT

The circulation in NL region is dominated by the south-eastward flowing Labrador Current system, which floods the eastern shelf areas with cold and relatively fresh subpolar waters (Figure 38). This flow can significantly affect physical and biological environments off Atlantic

Canada on seasonal and interannual time scales. On the shelf, the Coastal Labrador Current (Florindo-Lopez et al. 2020) originates near the northern tip of Labrador where the outflow from the Hudson Strait combines with the eastern Baffin Island Current and flows southeastward along the Labrador coast. During it southward journey on the on the Labrador shelf, is strongly influenced by the seabed topography, following the various cross shelf saddles and inshore troughs. A separate offshore branch of the Labrador Current flows southeastward along the western boundary of the Labrador Sea. This current is part of the large-scale Northwest Atlantic circulation consisting of the West Greenland Current that flows northward along the West Coast of Greenland, a branch of which turns westward and crosses the northern Labrador Sea forming the northern section of the Northwest Atlantic subpolar gyre.

Further south, near the northern Grand Bank, the Coastal Labrador Current becomes broader and less defined. In this region, most of the inshore flow combines with the offshore branch and flows eastward, with a portion of the combined flow following the bathymetry southward around the southeast Grand Bank, and the remainder continuing east and southward around the Flemish Cap (Figure 38). A smaller inshore component flows through the Avalon Channel and around the Avalon Peninsula, and then westward along the Newfoundland south coast. Off the southern Grand Bank the offshore branch flows westward along the continental slope, some of which flows into the Laurentian Channel and eventually onto the Scotian shelf. This extension of the Labrador Current on the Scotian shelf is referred to as the Scotian shelf break current. Additionally, there are strong interactions between the offshore branch of the Labrador Current and large-scale circulation. A significant portion of the offshore branch combines with the North Atlantic Current and forms the southern section of the subpolar gyre. Further east, the Flemish Cap is located in the confluence zone of subpolar and subtropical western boundary currents of the North Atlantic. Labrador Current water flows to the east along the northern slopes of the Cap and south around the eastern slopes of the Cap. In the eastern Flemish Pass, warmer high salinity North Atlantic Current water flows northward contributing to a topographically induced anticyclonic gyre over the central portion of the Cap.

Satellite altimetry data are used over a large spatial area to calculate the annual-mean anomalies of the Labrador Current transport (Han et al. 2014). A total of nine cross-slope satellite altimetry tracks are used to cover the Labrador Current on the NL shelf break from approximately 47°N to 58°N latitude (Figure 38). Similarly, five tracks from approximately 55°W to 65°W longitude are used for the Scotian shelf break current. The nominal cross-slope depth ranges used for calculating the transport are from 200 to 3,000 m isobaths over the NL shelf break and from 200 to 2,000 m isobaths over the Scotian shelf break.

An empirical orthogonal function (EOF) analysis of the annual-mean transport anomalies was carried out. An index was developed from the time series of the first EOF mode and normalized by dividing the time series by its SD. The mean transport values are provided based on ocean circulation model output along the NL shelf break (Han et al. 2008) and over the Scotian shelf break (Han et al.1997). The mean transport of the Labrador Current along the NL shelf break is 13 Sv (1 Sv = 10^6 m^3 s^{-1}) with a SD of 1.4 Sv, and the mean transport of the Scotian shelf break current is 0.6 Sv with a SD of 0.3 Sv. The mean transport values will be updated as new model output becomes available. The SD values will be updated as knowledge on nominal depth improves.

The Labrador Current transport along the NL shelf break was out of phase with that of the Scotian shelf break current for most of the years over 1993–2021 (Figure 39). The transport over the NL shelf break was strong in the early- and mid-1990s, weak in the mid-2000s and early-2010s, and became strong again in late 2010s. In contrast, the transport over the Scotian shelf break fluctuated in a nearly opposite way. The Labrador Current transport index was positively and negatively correlated with the winter NAO index over the NL and Scotian shelves breaks, respectively.

In 2021 the annual-mean transport of the Labrador Current over the NL shelf break continued the weakening trend that began in 2019 and became normal. The transport on the Scotian shelf break in 2021 remained below normal for eight consecutive years at -1.4 SD.

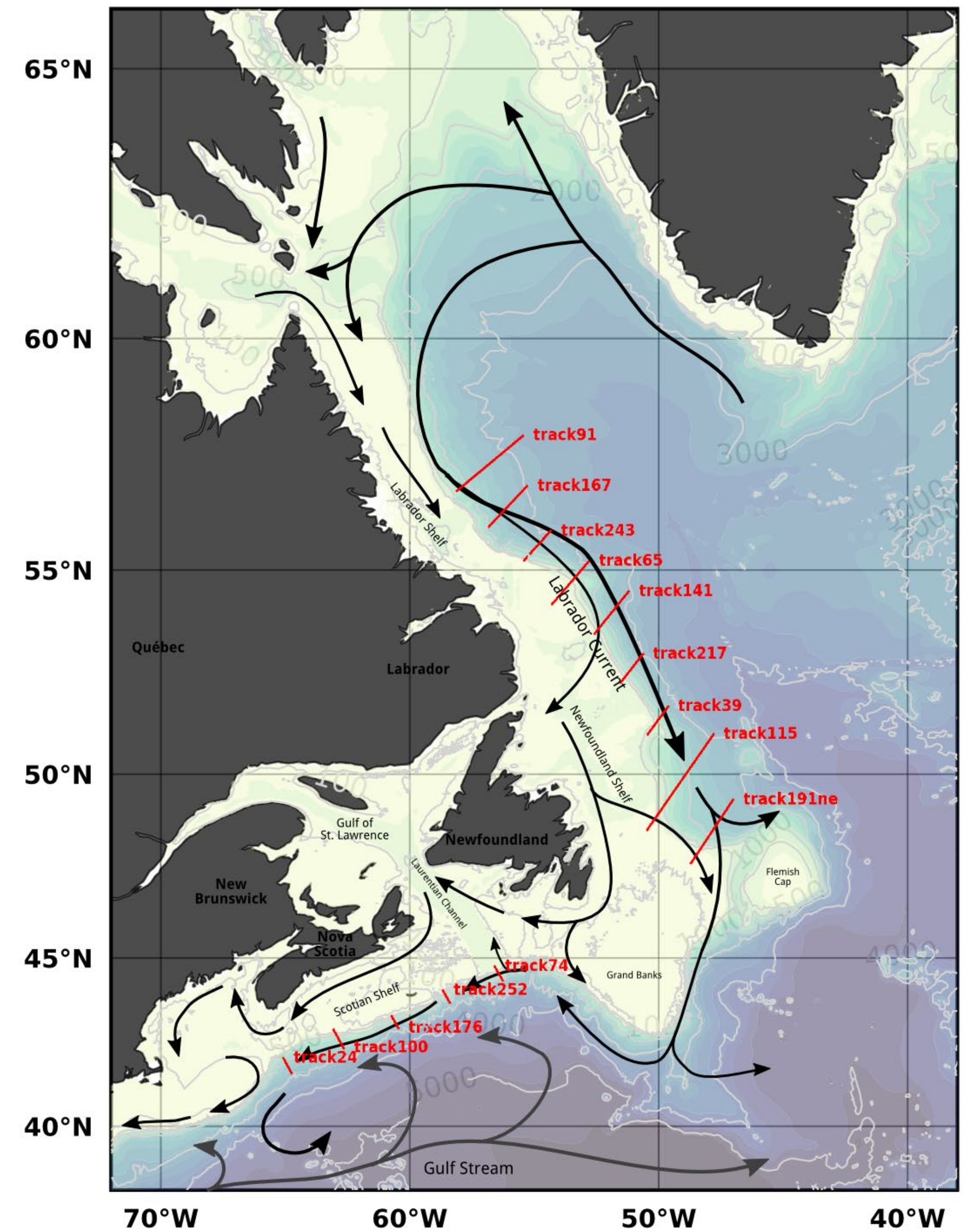

Figure 38: Map showing the Northwest Atlantic bottom topography (depth contour values in light gray) and schematic flow patterns (arrows). The transport is calculated across the cross-slope sections (red lines) identified by their satellite ground tracks numbers. The series of northern tracks are used for the Labrador Current calculation on the NL shelf, while the series of tracks in the south are used for the Scotian shelf break current transport.

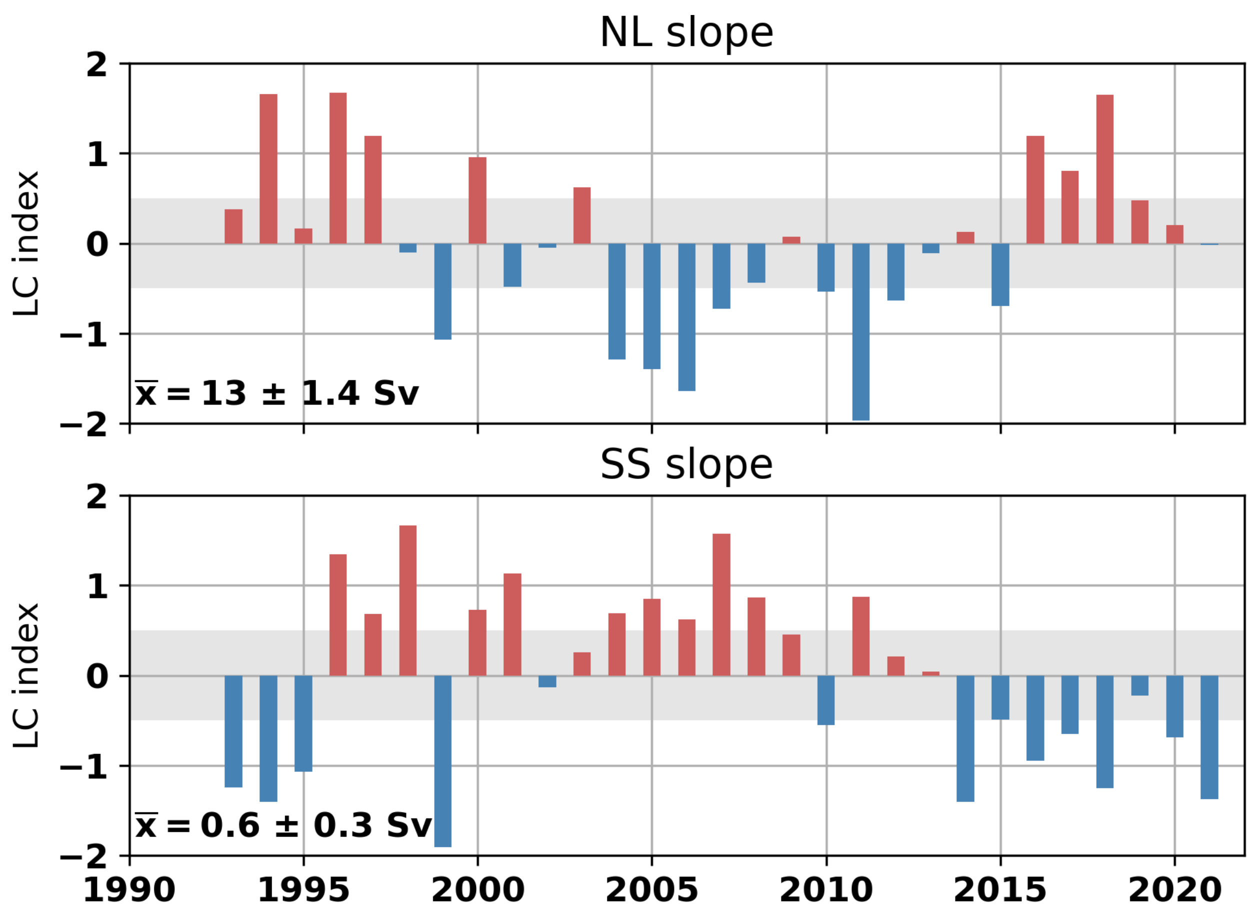

Figure 39: Normalized index of the annual-mean transport of the Labrador Current on the NL shelf break (top) and Scotian shelf break (bottom). Long-term averages over 1993–2021 (with standard deviation) are 13±1.4 Sv for the Labrador Current and 0.6±0.32 Sv for the Scotian shelf break current. Shaded gray areas represent the ±0.5 SD range considered "normal".

SUMMARY

The NL climate index (NLCI; Cyr and Galbraith 2021), summarizes selected time series discussed throughout this report (Figure 40). The NLCI runs between 1951 to present, and is updated annually. This index, presented here under the form of a scorecards followed by stacked bar plot of 10 equally weighted time series:

- Winter NAO index (starts in 1951; see Figure 3);
- Air temperatures at five sites (starts in 1950; see Figure 5);
- Sea ice season duration and maximum area for the northern Labrador, southern Labrador and Newfoundland shelves (starts in 1969; see Figure 12)
- Number of icebergs crossing 48°N (starts in 1950; see Figure 13);
- SSTs in NAFO Division 2GHJ3KLNOP (starts in 1982; see Figure 16);
- Vertically averaged temperature at Station 27 (starts in 1951; see Figure 19);
- Vertically averaged salinity at Station 27 (starts in 1951; see Figure 19);
- CIL core temperature at Station 27 (starts in 1951; see Figure 21);

- Summer CIL areas on the hydrographic sections Seal Island, Bonavista Bay and Flemish Cap (starts in 1950; see Figure 30); and
- Spring and fall bottom temperature in NAFO Divisions 3LNOPs and 2HJ3KLNO, respectively (starts in 1980; see Figure 37).

The NLCI can be interpreted as a measure of the overall state of the climate system with positive values representing warm and fresh conditions with less sea-ice and conversely negative values representing cold and salty conditions. It replaces the *Composite Environmental Index* (CEI) presented in similar reports on NL physical conditions until recently (e.g., Cyr et al 2019).

The NLCI highlights the different climate regimes prevailing since the early 1950s. For example, the 1960s stands out as the warmest period in the time series while the early 1990s is the coldest. The warming trend from the early 1990s that peaked in 2010 was followed by recent cooling that culminated in 2015. While the NLCI for years 2016 to 2020 were normal (with a certain spread between positive and negative anomalies), 2021 was one of the warmest years on record, at a record-high tied with 2010 and 1966. The NLCI its subindices are available at https://doi.org/10.20383/101.0301 (Cyr and Galbraith, 2020b).

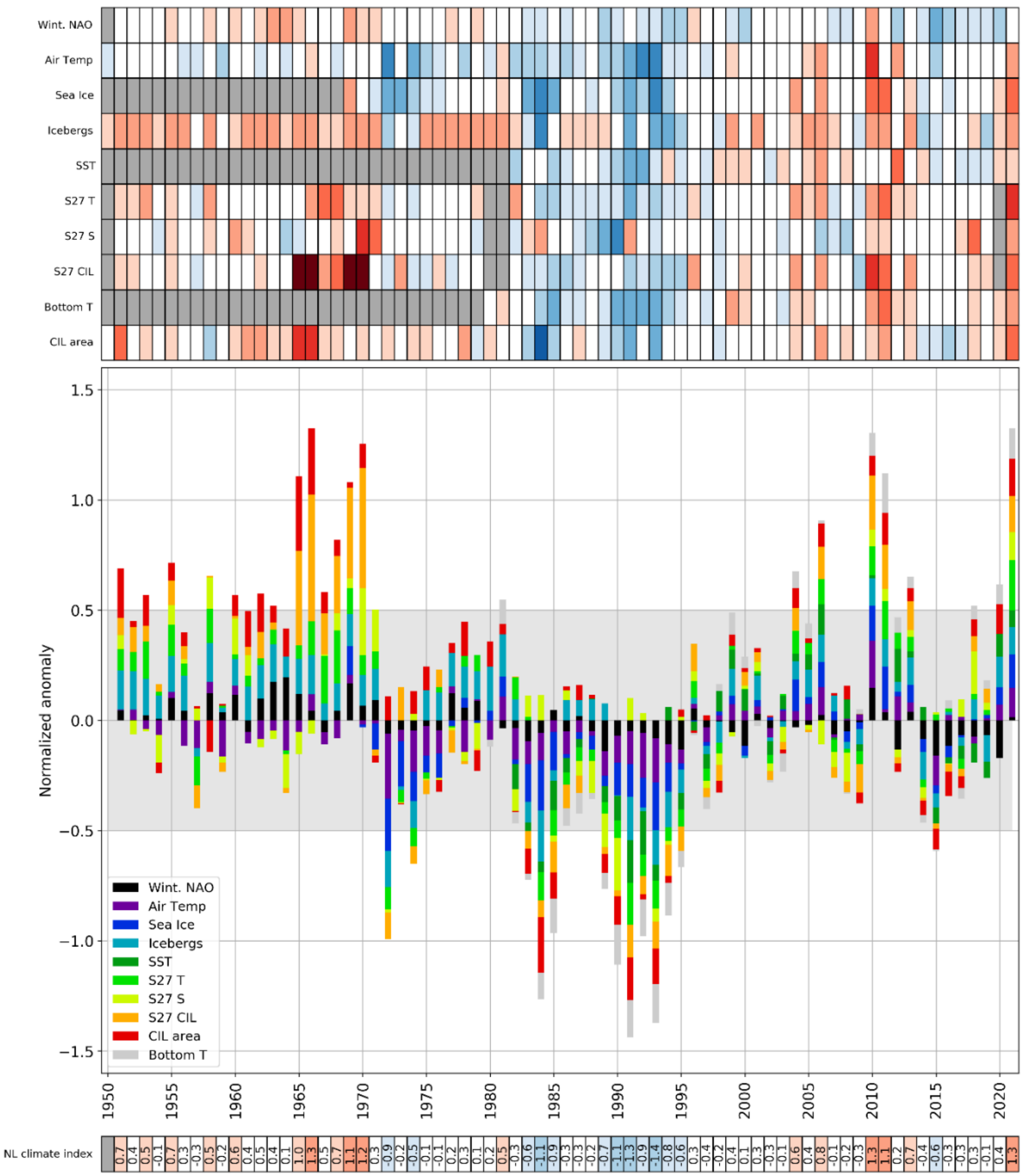

Figure 40: Newfoundland and Labrador climate index derived by averaging the normalized anomalies of various time series presented in this report. The scorecard in the top panel represents the 10 subindices used to construct the climate index, color-coded according to their value (blue negative, red positive, white neutral). The sign of some indices (NAO, ice, icebergs, salinity and CIL volume) has been reversed when positive anomalies are generally indicative of colder conditions. Grey cells in the scorecards indicate the absence of data. The central panel represents the climate index in a stacked-bar fashion, in which the total length of the bar is the average of the respective subindices and in which their relative contribution to the average is adjusted proportionally. The scorecard at the bottom of the figure shows the color-coded numerical values of the climate index.

HIGHLIGHTS OF 2021

- Based on the NL climate index, 2021 was one of the warmest years on record (tied with 2010 and 1966).
- The annual air temperature at 5 sites around the NW Atlantic was at its second warmest level of the time series (started in 1950) after 2010. New records were however set for the winter air temperature in Iqaluit, Bonavista and St. John's (tied with 2011).
- Sea ice conditions (season duration and maximum cover) were at their third lowest level of the time series (started in 1969), after 2010 and 2011.
- Only one iceberg drifted south of 48°N, one of the lowest number of all time (one was also observed in 2010, while none were observed in 2006 and 1966).
- Vertically-averaged temperature at Station 27 was at a series record-high (started in 1951).
- Vertically-averaged salinity at Station 27 was at its second freshest level (after 2018) since the great salinity anomaly of the early 1970s.
- The CIL cross-sectional area averaged over 3 hydrographic sections on the NL shelf was the third smallest on record (series started in 1950) after 1966 and 1965, respectively.
- The bottom temperatures averaged over the spring (3Ps) and fall (2HJ3K) were the second warmest of time series after 2011 (series started in 1980).
- The transport on the Scotian Slope remained below normal for an eighth consecutive year.

ACKNOWLEDGEMENTS

This work is a contribution to the scientific program of the Atlantic Zone Monitoring Program. We thank the many scientists and technicians at the Northwest Atlantic Fisheries Centre for collecting and providing much of the data contained in this analysis and the Marine Environment Data Section of Fisheries and Oceans Canada in Ottawa for providing most of the historical data. We also thank the captain and crew of the CCGS Teleost for oceanographic data collection during the summer of 2021. We thank Heather Andres and Jared Penney for reviewing the document.

REFERENCES CITED

Colbourne, E., Holden, J., Senciall, D., Bailey, W., Craig, J., and S. Snook. 2015. Physical Oceanographic Conditions on the Newfoundland and Labrador Shelf during 2014. DFO Can. Sci. Advis. Sec. Res. Doc. 2015/053. v + 37 p.

Colbourne, E.B., Narayanan, S., and Prinsenberg, S. 1994. Climatic changes and environmental conditions in the Northwest Atlantic, 1970-1993. ICES Mar. Sci. Symp. 198:311–322.

Cyr, F., Colbourne, E., Holden, J., Snook, S., Han, G., Chen, N., Bailey, W., Higdon, J., Lewis, S., Pye, B. and D. Senciall. 2019. Physical Oceanographic Conditions on the Newfoundland and Labrador Shelf during 2017. DFO Can. Sci. Advis. Sec. Res. Doc. 2019/051. iv + 58 p.

Cyr, F., Snook, S., Bishop, C., Galbraith, P.S., Pye, B., Chen, N., and Han, G. 2021 Physical Oceanographic Conditions on the Newfoundland and Labrador Shelf during 2019. DFO Can. Sci. Advis. Sec. Res. Doc. 2021/017. iv + 52 p.

Cyr, F. and Galbraith, P. 2020a. Newfoundland-Labrador Shelf. Ch. 4.3 in: ICES Report on Ocean Climate 2019 (González-Pola, C., Larsen, K.M.H., Fratantoni, P., and Beszczynska-Möller, A. [Eds.]). 2020. ICES Cooperative Research Reports No. 350. 136 pp.

Cyr, F. and Galbraith, P. 2020b. Newfoundland and Labrador climate index. Federated Research Data Repository. Version 2021.

Cyr, F. and Galbraith, P.S. 2021. A climate index for the Newfoundland and Labrador shelf. Earth Syst. Sci. Data. 13(5):1807–1828.

Dickson, R.R., Meincke, J., Malmberg, S-A., and Lee, A.J. 1988. The "great salinity anomaly" in the Northern North Atlantic 1968–1982. Prog. Oceanogr. 20(2):103–151.

Doubleday, W.G., Editor. 1981. Manual on Groundfish Surveys in the Northwest Atlantic. NAFO. Sci. Coun. Studies. 2:7–55.

Drinkwater, K.F. 1996. Atmospheric and Oceanic Variability in the Northwest Atlantic During the 1980s and Early 1990s. J. Northw. Atl. Fish. Sci. 18:77–97.

Florindo-López, C., Bacon, S., Aksenov, Y., Chafik, L., Colbourne, E., and Holliday, N.P. 2020. Arctic Ocean and Hudson Bay Freshwater Exports: New Estimates from Seven Decades of Hydrographic Surveys on the Labrador Shelf. J. Clim. 33(20):8849–8868.

Galbraith, P.S., Larouche, P., and Caverhill, C. 2021. A Sea-Surface Temperature Homogenization Blend for the Northwest Atlantic. Can. J. Remote Sens. 47(4):554–568.

Han, G., Chen, N., and Ma, Z. 2014. Is there a north-south phase shift in the surface Labrador Current transport on the interannual-to-decadal scale? J. Geophys. Res. Oceans. 119(1):276–287.

Han, G., Lu, Z., Wang, Z., Helbig, J., Chen, N., and de Young, B. 2008. Seasonal variability of the Labrador Current and shelf circulation off Newfoundland. J. Geophys. Res. Oceans. 113(C10):1–23.

Han, G., Hannah, C.G., Loder, J.W., and Smith, P.C. 1997. Seasonal variation of the three-dimensional mean circulation over the Scotian Shelf. J. Geophys. Res. Oceans. 102(C1):1011–1025.

ICNAF. 1978. List of ICNAF standard oceanographic sections and stations. ICNAF selected papers #3. NAFO.

International Ice Patrol. 1995. International Ice Patrol (IIP) Iceberg Sightings Database, Version 1. Boulder, Colorado USA. NSIDC: National Snow and Ice Data Center. doi. [Accessed 2022-01-18].

Kerr, R.A. 2000. A North Atlantic Climate Pacemaker for the Centuries. Science 288(5473):1984–1985.

McDougall, T.J. and Barker, P.M. 2011: Getting started with TEOS-10 and the Gibbs Seawater (GSW) Oceanographic Toolbox, 28pp., SCOR/IAPSO WG127, ISBN 978-0-646-55621-5.

Petrie, B., Pettipas, R.G., and Petrie, W.M. 2007. An Overview of Meteorological, Sea Ice and Sea-Surface Temperature Conditions off Eastern Canada during 2006. DFO Can. Sci. Advis. Sec. Res. Doc. 2007/022. iii + 38 p.

Petrie, B., Akenhead, S., Lazier, J., and Loder, J. 1988. The Cold Intermediate Layer on the Labrador and Northeast Newfoundland Shelves, 1978–86. NAFO Sci. Coun. Studies. 12:57–69.

Therriault, J.-C., Petrie, B., Pepin, P., Gagnon, J., Gregory, D., Helbig, J., Herman, A., Lefaivre, D., Mitchell, M., Pelchat, B., Runge, J., and Sameoto, D. 1998. Proposal for a Northwest Atlantic Zonal Monitoring Program. Can. Tech. Rep. Hydrogr. Ocean Sci. 194: vii + 57 p.

Thyng, K.M., Greene, C.A., Hetland, R.D., Zimmerle, H.M., and DiMarco, S.F. 2016. True colors of oceanography: Guidelines for effective and accurate colormap selection. Oceanography. 29(3):9–13.

Vincent, L.A., Wang, XL., Milewska, E.J. Wan, H., Yang, F., and Swail, V. 2012. A second generation of homogenized Canadian monthly surface air temperature for climate trend analysis. J. Geophys. Res. Atmospheres. 117(D18).